THE ASTROPHYSICAL JOURNAL, 419:318–336, 1993 December 10

THE ACCRETION DISK LIMIT CYCLE MODEL: TOWARD AN UNDERSTANDING OF THE LONG-TERM BEHAVIOR OF SS CYGNI

JOHN K. CANNIZZO[1]
NASA/GSFC, Laboratory for Astronomy and Solar Physics, Code 681, Greenbelt, MD 20771
Received 1993 May 12; accepted 1993 June 10

ABSTRACT

We present detailed computations of the limit cycle model for dwarf nova outbursts with application to SS Cygni, the best studied dwarf nova. We examine how secular changes in the input parameters of the model affect the properties associated with the outbursts. For input parameters which reproduce the observed outburst recurrence times and outburst durations for SS Cyg, our time-dependent, accretion disk instability code generates light curves in which one or more short outbursts tend to be sandwiched between two long outbursts. We find that the relative frequency of long versus short outbursts can be influenced by changes in the accretion disk viscosity and mass transfer rate. By forming moving averages taken from the long-term AAVSO light curve of SS Cyg, we find a strong correlation between the recurrence time for outbursts t_c and the ratio of the number of long outbursts $N(\mathrm{L})$ to the number of short outbursts $N(\mathrm{S})$ occurring in a given time interval. This can be accounted for in the model in several ways. Changes in the radius of the inner edge of the disk produce correlated changes in t_c and $N(\mathrm{L})/N(\mathrm{S})$, as do slow variations in either α_{cold} or α_{hot}—the accretion disk viscosity parameters in quiescence and outburst. In this latter scenario, there must be a fundamental asymmetry between the two alphas in the sense that both quantities cannot be varying in step with each other—i.e., one must remain fixed while the other varies. Finally, variations in the mass transfer rate $\dot{M}_T$ cannot directly account for the observed long-term changes in the light curve of SS Cyg as was postulated by Hempelmann & Kurths and by Cannizzo & Mattei.

Subject headings: accretion, accretion disks — novae, cataclysmic variables — stars: individual (SS Cygni)

1. INTRODUCTION

The accretion disk limit cycle mechanism successfully accounts for the outbursts seen in the dwarf novae, a subclass of the cataclysmic variables. The impetus for the model was provided by Osaki (1974), and later workers found a physical basis for having a limit cycle operating in an accretion disk (Meyer & Meyer-Hofmeister 1981; Smak 1982; Cannizzo, Ghosh, & Wheeler 1982; Mineshige & Osaki 1983, hereafter MO83; Faulkner, Lin, & Papaloizou 1983, hereafter FLP; see also Wesselink 1939). For a recent review see Cannizzo (1993). The time-dependent modeling to date has explored the behavior of the outburst light curves using constant input parameters. No time-dependent study has been carried out in which such quantities as the secondary mass transfer rate $\dot{M}_T$ or the accretion disk viscosity parameter α were made to vary during the course of a numerical run. Recently, Cannizzo & Mattei (1992, hereafter CM) studied the long-term visual light curve of SS Cygni taken by the American Association of Variable Star Observers (AAVSO). They studied the long-term moving averages of the timescales associated with the outbursts and noted an inverse relation between the quiescent flux and the recurrence time for outbursts by comparing the fluctuations in these two quantities on very long timescales. (This relation had been commented on previously by Warner 1987.) CM drew several conclusions based on general results from previous theoretical studies (Cannizzo, Shafter, & Wheeler 1988, hereafter CSW; Duschl & Livio 1989, hereafter DL). The model input parameters for these earlier works had not, however, been tuned to reproduce the light curve of a specific system, and, as mentioned earlier, variable input parameters were not considered. In light of the wealth of long-term data on SS Cyg and the findings of CM, it now becomes interesting to perform time-dependent computations with varying control parameters to study in detail what constraints we can place on the model. The primary constraints are on α_{cold} and α_{hot}, and these come from the observed timescales for the duration of outbursts and the recurrence time for outbursts. By trying to match observed correlations between fluctuations in such quantities as the mass transfer rate from the secondary star and the outburst timescales, we gain potential information on the interrelationships among the different physical parameters. These can lead, in turn, to constraints on the underlying accretion dsk physics.

Our study has an advantage over previous time-dependent accretion disk studies in that we are searching for *differential* effects—i.e., how slow changes in the control parameters for the model affect the light curves. Previous studies were primarily concerned with obtaining a definite number, such as the time delay between the onset of the dwarf nova outburst at optical and UV wavelengths (e.g., Smak 1984; Cannizzo, Wheeler, & Polidan 1986; Pringle, Verbunt, & Wade 1986; Cannizzo & Kenyon 1987; Mineshige 1988; Meyer & Meyer-Hofmeister 1989; Meyer 1991; Livio & Pringle 1992). Studies which strive to obtain a specific number with which to compare to observations are invariably biased by their input physics, many aspects of which are poorly known in accretion disks. In particular, the size of the UV delay is affected by assumptions regarding the detailed shape of the viscosity–surface density relation for the accretion disk, the evolution of the inner disk during quiescence, the annular flux distributions for the disk (e.g., Planckian vs. stellar/Kurucz), and other physics. While our study is subject to these same uncertainties, the *changes* in the model light curves for successive outbursts

[1] NRC Senior Research Associate.

brought about by introducing a change to an input parameter (a change which occurs on a much longer timescale than the outburst recurrence time) should be less sensitive to details of the input physics. Thus, although the specific values of quantities such as the outburst recurrence time and outburst duration cannot be taken too literally, the secular changes which we find should be fairly robust.

Section 2 contains a description of our numerical model, § 3 gives the results of runs using various assumptions about the input physics, § 4 contains a discussion of the results in the context of the observational data on SS Cyg, § 5 discusses the implications of our findings for dwarf novae in general, and § 6 sums up.

2. THE NUMERICAL MODEL

We follow the time evolution of the accretion disk by solving for the surface density $\Sigma(r, t)$ and midplane (or "vertically averaged") temperature $T(r, t)$. The governing equations are

$$\frac{\partial \Sigma}{\partial t} = \frac{3}{r}\frac{\partial}{\partial r}\left[r^{1/2}\frac{\partial}{\partial r}(r^{1/2}\nu\Sigma)\right] + S(\Sigma) \quad (1)$$

and

$$\frac{\partial T}{\partial t} = \frac{2(H - C + J)}{c_p \Sigma} - \frac{\mathscr{R}T}{\mu c_p}\frac{1}{r}\frac{\partial (rv_r)}{\partial r} - v_r\frac{\partial T}{\partial r}, \quad (2)$$

where $\nu = (2/3)(\alpha\mathscr{R}T/\mu\Omega)$ is the viscosity coefficient, S is a mass addition term to account for matter arriving from the secondary star, $v_r = -(3\nu/r)\partial \log (\nu\Sigma r^{1/2})/\partial \log r$ is the local (radial) flow velocity of matter, $H = (9/8)\nu\Omega^2\Sigma$ and $C = \sigma T^4$ are the viscous heating and radiative cooling terms, and $J = (3/2)c_p\nu(\Sigma/r)[\partial(r\,\partial T/\partial r)/\partial r]$ represents the radial energy flux carried by viscous processes (cf. FLP; Smak 1984; MO83; Mineshige 1986; Ichikawa & Osaki 1992). The more standard radial flux term given by FLP, $J = -(h/r)[\partial(rF_r)/\partial r]$, where $F_r = -[4acT^3/(3\kappa\rho)](\partial T/\partial r)$, gives the heat flux due to radiative diffusion rather than viscous diffusion. In tests, we find the two terms to be comparable in magnitude, but the FLP expression is more prone to numerical problems because of its high temperature dependence. We therefore adopt the viscous transport term (Mineshige 1986). The thermal equation is necessary for following the movement of the heating and cooling fronts which travel back and forth through the disk and bring about the transitions between the two allowed viscosity states. The term in equation (2) involving $\partial(rv_r)/\partial r$ represents the energy release from $P\,dV$ work, and the final term (containing $\partial T/\partial r$) characterizes the advective transport of energy contained in the matter which flows across the hot/cold transition (FLP; Ichikawa & Osaki 1992).

As previously, we divide our numerical grid into N points equally spaced in $\sqrt{r}$ as per Bath & Pringle (1981). Our inner boundary condition is that $\Sigma(r_{\rm inner}) = 0$, and at the outer edge we continually adjust the $\Sigma(r)$ profile (while conserving mass) so that $v_r = 0$. In order to save on computer time, we do not include in equations (1) and (2) the effects of tidal heating and tidal torque from the secondary star. Our condition $v_r = 0$ corresponds to having a "brick wall" or tidal-like force of the form $F \propto (r/r_{\rm outer})^{\eta}$, where $\eta \to \infty$. Other workers (e.g., Ichikawa & Osaki 1992) have shown how a realistic treatment of the torque leads to variations in the outer disk radius. For bursts starting at large radii in the accretion disk, the interplay between the outward flow of angular momentum within the disk and the tidal torque at the outer edge leads to a rapid expansion during burst onset, and a slow contraction of the disk during quiescence. This effect is especially important for the short orbital period systems studied by Ichikawa & Osaki because the secondary mass $M_2 \propto P_{\rm orbital}$ and the primary mass $M_1 \simeq 1\ M_\odot$. For a CV with a mass ratio $q = M_1/M_2$ greater than about 3, the tidal torque on the disk is expected to increase dramatically when the outer edge expands beyond the 3:1 orbital resonance radius. For SS Cyg, however, $q \sim 1$, and furthermore, we will see that for SS Cyg parameters, the outbursts begin at small radii in the disk; therefore, the changes in disk radius during the limit cycle should be less drastic than for systems exhibiting "outside-in" bursts. In addition, we are primarily concerned with the long-term behavior of the optical light from the disk—the properties of the outbursts—and changes in the disk radius are a secondary effect.

Many improvements have been incorporated into the time-dependent thermal instability code (used earlier by Cannizzo 1984; Cannizzo et al. 1986; Cannizzo & Kenyon 1986, 1987; and Huang & Wheeler 1989). One shortcoming of the earlier versions involved the times of phase transitions between the two stable states: During the times of heating the cooling term was set to zero, and during times of cooling the heating term was set to zero. Other workers have determined the evolution in a more self-consistent fashion by following the evolution of the midplane temperature and using a tabular or analytical relation for the effective temperature $T_e = T_e(T, r, \Sigma)$. This is the method we now follow. Also, we adopt the convention given by Ichikawa & Osaki (1992) for calculating T_e during times when the temperature of an annulus is intermediate between the cold and hot state. We take

$$\log(\sigma T_e^4) = \psi\{\log[\sigma T_e^4(\Sigma_{\rm max})] - \log[\sigma T_e^4(\Sigma_{\rm min})]\} + \log[\sigma T_e^4(\Sigma_{\rm min})], \quad (3)$$

where

$$\psi = \frac{\log[T/T(\Sigma_{\rm min})]}{\log[T(\Sigma_{\rm max})/T(\Sigma_{\rm min})]}, \quad (4)$$

and $\Sigma_{\rm min}$ and $\Sigma_{\rm max}$ represent the surface densities at the local minimum and maximum, respectively, in the S-curve determined from the computations of the vertical structure of the disk.

By considering in proper detail the physics associated with the transition fronts, Mineshige (1988) found a "stagnation" effect which comes about when the temperature of the gas in a given annulus is just hotter than $\sim 10^4$ K. The stagnation slows the heating and cooling processes considerably over what was found in studies using simplified treatments of the energy equation (e.g., Pringle et al. 1986; Cannizzo & Kenyon 1987).

Stagnation has three primary elements:

1. The specific heat increases greatly for gas at $10^4 \lesssim T(\mathrm{K}) \lesssim 1.5 \times 10^4$. The addition or subtraction of a given amount of heat goes almost exclusively into changing the ionization state of the gas and does not significantly affect the temperature.

2. The local maximum in the S-curve (of steady state solutions, plotted as $\log T_e$ vs. $\log \Sigma$) is rounded, whereas the local minimum is sharp. This can be seen in the vertical structure studies (e.g., MO83; Cannizzo & Wheeler 1984, hereafter CW; Pojmański 1986). The slowly changing slope of the S-curve in the vicinity of $\Sigma_{\rm max}$ causes the difference between the heating

and cooling functions to be small when an annulus first begins to heat. Since the thermal time is much shorter than the viscous time, the annulus at first heats while maintaining roughly constant surface density. (Mineshige 1988 estimates that $[H - C]/H \sim 0.1$ for a significant amount of time during the onset of instability.)

3. There is an intermediate stable branch of solutions between the well-known lower and upper branches upon which an annulus may rest during the course of heating.

These three effects are important during the onset of a heating transition and during the end of the cooling transition within a given annulus, and they can affect the shapes of the rise and decay portions of the computed outbursts. In this study we are more interested in the long-term behavior of the disk, so the stagnation is not critical to our model. In addition, effects (2) and (3) are somewhat dependent on the input physics to the vertical structure computations. The third effect is very dependent on the choice of the mixing length in the treatment of convection, and also the specific functional form and numerical value of $\alpha_{\rm cold}$. The rounded maximum seems to be a more universal feature of the vertical structure computations, however, given our uncertainty about such effects as convection in a highly shearing medium, the deposition of viscous heating within the vertical structure, and the treatment of molecular and dust absorbers in the quiescent state, we model the S-curve as consisting merely of two different power-law expressions—one for the upper branch and one for the lower branch—and thus we do not take account of variations in $d \log T_e/d \log \Sigma$ near the local extrema in the S-curve. We have decided to include only the first stagnation effect (involving the specific heat). Indeed, we have found during the course of our numerical experimentation that, by simply taking $c_p/(\mathscr{R}/\mu)$ to be a constant of order unity (as was done, e.g., by Pringle et al. 1986 and Cannizzo & Kenyon 1987) in the current version of our model, the cooling wave propagates too quickly during the outburst decay phase, and the rapid outflux of heat carried by matter crossing the hot/cold interface causes the cooling wave to be reflected as a heating wave. One does not obtain well-separated outbursts, but rather the transition fronts constantly run back and forth through approximately the outer one-half of the disk, and the resulting light curve has a sawtooth pattern.

To expedite the computations we utilize a simple analytical fit for the specific heat c_p. Figure 1 shows c_p (in terms of $\mathscr{R}/\mu$) for $\log \rho(\mathrm{g\ cm^{-3}}) = -8$, -7, and -6 obtained using a subroutine written by H. Saio which is based on the physics described in Iben (1963). Also shown are curves using the Gaussian fit

$$\frac{c_p(\rho, T)}{\mathscr{R}/\mu} = 2.7 + Ae^{-(\log T - \log T_0)^2/w^2}, \tag{5}$$

where $A = 26 - 7(\log \rho + 7)$, $\log T_0 = 4.1 + 0.07(\log \rho + 7)$, and $w = 0.115 + 0.015(\log \rho + 7)$. Except for a slight shoulder in c_p in the physically realistic curves at $\log T \sim 4.2$–4.4 due to He ionization, the agreement between the two sets of curves is good.

The parameterization of the steady state physics embodied in the S-curve is based on the results of CW. All the information concerning the specific shape of the S-curve enters through the scaling for the effective temperature. The high state of the disk is easy to parameterize in terms of the standard, vertically averaged scalings (Shakura & Sunyaev 1973).

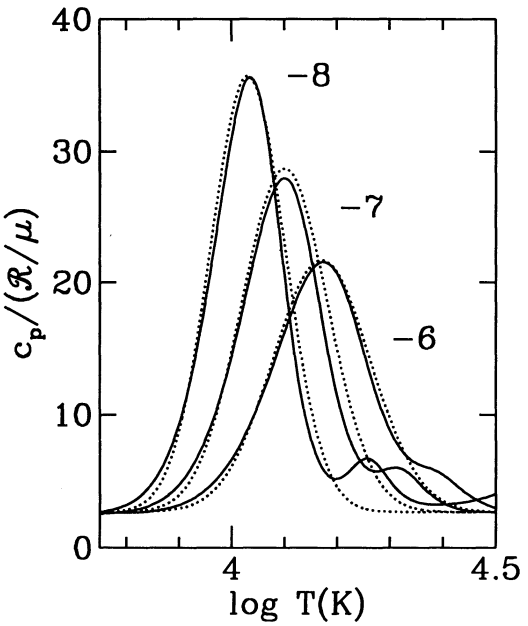

FIG. 1.—The specific heat c_p vs. temperature for $\log \rho = -8$, -7, and -6 as given by the subroutine PEDET written by Hideyuki Saio. The three dashed curves come from the fitting formula given in the text.

That the vertically averaged approach and the assumption of radiative transfer are valid, in particular that $T^4 \sim \tau T_e^4$ (where τ is the optical depth through the vertical structure), was quantitatively shown by Cannizzo (1992). Cannizzo calculated a parameter $s \equiv \tau T_e/T^4$ determined from vertical structure computations, and found that $s \sim 1$ on the upper branch of the S-curve, but that s can become quite large along the lower branch of the S. This is especially true for disks with small alpha values such as are inferred to exist in the quiescent state of dwarf novae. Our approach in formulating power law scalings for the midplane and photospheric values of the temperature (T and T_e) along the S-curve is therefore to use Shakura & Sunyaev–like vertically averaged scalings for the hot state, and to take the results from vertical structure computations for the low state. As mentioned earlier, we characterize the upper and lower branches of the S-curve each by a single power law $T_e = T_e(T, r, \Sigma)$.

The turning points in the S-curve determined from the vertical structure computations define the minimum and maximum in surface density Σ. We use the values determined by CW which are as follows

$$\Sigma_{\rm max} = 11.4\ \mathrm{g\ cm^{-2}}\ r_{10}^{1.05} m_1^{-0.35} \alpha_{\rm cold}^{-0.86}, \tag{6}$$

$$\Sigma_{\rm min} = 8.25\ \mathrm{g\ cm^{-2}}\ r_{10}^{1.05} m_1^{-0.35} \alpha_{\rm hot}^{-0.8}, \tag{7}$$

$$T_{e,\rm max} \equiv T_e(\Sigma_{\rm max}) = 5870\ \mathrm{K}\ r_{10}^{-0.1}, \tag{8}$$

and

$$T_{e,\rm min} \equiv T_e(\Sigma_{\rm min}) = 7951\ \mathrm{K}(m_1/r_{10}^3)^{0.05}, \tag{9}$$

where $r_{10} = r/10^{10}$ cm, $m_1 = M_{\rm WD}/1M_\odot$, $\alpha_{\rm cold}$ is the value of α along the lower stable branch of solutions, and $\alpha_{\rm hot}$ is the value of α along the upper stable branch of solutions.

For the high state, we take equations (A6) and (A7) from Cannizzo & Reiff (1992), and the opacity law $\kappa = 2.8 \times 10^{24} \rho T^{-3.5}$ cm^2 g^{-1} (eq. [3.14] from CSW) to

obtain

$$T(\text{hot}) = 9755 \text{ K } m_1^{1/7} r_{10}^{-3/7} \alpha_{\text{hot}}^{1/7} \Sigma^{3/7} \mu_{\text{hot}}^{-1/14} \quad (10)$$

and

$$T_e(\text{hot}) = 3334 \text{ K } m_1^{9/56} r_{10}^{-27/56} \alpha_{\text{hot}}^{2/7} \Sigma^{5/14} \mu_{\text{hot}}^{-15/56} . \quad (11)$$

Eliminating α gives

$$T_e(\text{hot}) = 35{,}040 \text{ K } m_1^{-1/8} r_{10}^{3/8} \Sigma_2^{-1/2} \mu_{\text{hot}}^{-1/8} T_5(\text{hot})^2 , \quad (12)$$

where $\Sigma_2 = \Sigma/100 \text{ g cm}^{-2}$ and $T_5(\text{hot}) = T(\text{hot})/10^5$ K.

The low state of the S-curve is subject to many uncertainties of input physics. The best one can do in time-dependent computations is to use the results of existing vertical structure computations, while keeping in mind their limitations. Cannizzo & Kenyon (1987) parameterized the low state of the accretion disk as four power-law segments of $T_e(\Sigma, \alpha, r)$. This was motivated by the computations of CW—in particular the fourth curve in Figure 11 of CW representing the low state for $\alpha = 0.032$. As shown by MO83, Pojmański (1986), and Cannizzo (1992), however, the shape of the track of solutions near Σ_{max} is quite dependent on the assumed efficiency of convection (usually expressed in terms of the mixing length as $l = \gamma \min [z, H_P]$, where γ is an adjustable parameter of order unity, z is height above midplane, and H_P is the pressure scale height in the disk). The dependency of the vertical structure on γ becomes stronger as α_{cold} is made smaller. In view of uncertainties regarding convection and the opacity at low temperatures, we adopt a single power law for the low state $T_e(\text{cold}) = B\Sigma^{0.75}\alpha_{\text{cold}}^{b} r_{10}^{-c}$. The Σ exponent comes from a rough fit using Figure 11 of CW and corresponds to an optically thick disk in quiescence. Most time-dependent studies adopt quiescent physics which assumes the disk to be optically thin in the continuum in the visual band (e.g., Lin, Papaloizou, & Faulkner 1985, hereafter LPF; Meyer & Meyer-Hofmeister 1984; Mineshige & Osaki 1985; Ichikawa & Osaki 1992). We believe, however, that there are strong arguments in favor of an optically thick quiescent disk underlying an optically thin chromosphere (Cannizzo 1993). Also, we take our scaling for Σ_{max} from the local maximum associated with the convection effect, not the one produced by the opacity effect (MO83; CW; Cannizzo 1993).

We may infer the constants B, b, and c by evaluating $T_e(\text{cold})$ at the termination of the quiescent branch $\Sigma = \Sigma_{\text{max}}$ using equation (6), and setting $T_e(\text{cold})$ equal to T_e in equation (8). By matching the coefficient and the exponents we obtain

$$T_e(\text{cold}) = 946 \text{ K } \Sigma^{0.75} \alpha_{\text{cold}}^{0.645} r_{10}^{-0.8875} . \quad (13)$$

Using $(9/8)\nu\Omega^2\Sigma = \sigma T_e^4$ and eliminating α_{cold} we obtain our $T_e(T, r, \Sigma)$ scaling

$$T_e(\text{cold}) = 5505 \text{ K } \Sigma_2^{-0.664} T_4(\text{cold})^{0.4082} r_{10}^{-0.0506} . \quad (14)$$

Finally, we may combine the previous equations to get

$$T_{\text{max}} \equiv T(\Sigma_{\text{max}}) = 8219 \text{ K } r_{10}^{0.05} \alpha_{\text{cold}}^{0.14} \quad (15)$$

and

$$T_{\text{min}} \equiv T(\Sigma_{\text{min}}) = 39387 \text{ K } \alpha_{\text{hot},-1}^{-0.2} , \quad (16)$$

where $\alpha_{\text{hot},-1} = \alpha_{\text{hot}}/0.1$.

Most previous studies have found that, in order to produce well-separated outbursts, α must be larger along the upper branch of the S-curve than along the lower branch. (It is quite conceivable that future revisions of the vertical structure will affect the scalings given above so that α = constant may be allowed.) Many studies have taken α to be some monotonically increasing function of h/r or T. In this work we are primarily interested in studying how changes in the input parameters such as α and $\dot{M}_T$ affect the behavior of the light curves; therefore we prefer to have α vary in a step function from the lower to the upper branches. (When an annulus is heating or cooling, we interpolate $\alpha[T]$ between α_{cold} and α_{hot} based on T_{max}, T, and T_{min}.) That we have a well-defined α_{cold} and α_{hot} makes it easier to disentangle the final results from the many competing effects which are always operating simultaneously within a given run.

3. NUMERICAL EXPERIMENTATION

3.1. *Standard Model*

The basic parameters required in the disk instability model to reproduce the observed timescales associated with the outbursts in SS Cyg are $\alpha_{\text{cold}} \cong 0.02$, $\alpha_{\text{hot}} \cong 0.1$, and $\dot{M}_T \cong 10^{-9} M_\odot \text{ yr}^{-1}$ (Cannizzo et al. 1986; Cannizzo & Kenyon 1987). We add the mass arriving from the secondary star in a Gaussian distribution near the outer edge. We take $r_{\text{outer}} = 4 \times 10^{10}$ cm, $r_{\text{inner}} = 5 \times 10^8$ cm, $r_{\text{add}} = 3.5 \times 10^{10}$ cm, and $r_{\text{FWHM}} = 10^9$ cm. These radii represent the outer and inner disk radii, the point of mass addition, and the full width at half-maximum of the Gaussian for mass addition. Bath & Pringle (1981, 1982) describe a method of adding mass at the outermost grid points and having it settle down to smaller radii while sweeping up mass and angular momentum. Since so much mass is always present in the outer disk in our computations, this method always gives an r_{add} only slightly interior to r_{outer}. For convenience we fix $r_{\text{add}} = 0.875 r_{\text{outer}}$ and adopt the smoothing length r_{FWHM}. During the course of numerical experimentation, we find our computed light curves to be insensitive to the method of mass addition. For example, decreasing r_{FWHM} by a factor of 100 produces no noticeable affect on the light curves, nor does switching to using the method of Bath & Pringle. This seems to come about because the intrinsic viscous spreading in the disk naturally broadens a narrow annulus into a wider one. Hence, the torus of enhanced surface density at large radii produced by the addition of mass cannot be made narrow. Also, for SS Cyg parameters our outbursts are triggered at small radii in the disk, and the specific surface density profile which exists at larger radii at the onset of thermal instability is erased by the subsequent heating front.

To compute the visual magnitude m_v of the system, we assume a face-on accretion disk at a distance of 100 pc. Each annulus is taken to emit a Planckian spectrum, so that

$$m_v = -2.5 \log (f_v) + 99.01 , \quad (17)$$

where

$$f_v = \sum_{i=1}^{N} \sum_{j=1}^{11} w(j) \frac{\delta\lambda/\lambda(j)^5}{[\![\exp \{hc/[\lambda(j) k T_e(r_i)]\} - 1]\!]} r_i \times (r_i - r_{i-1}) . \quad (18)$$

The two sums are over the radial grid (i index) and wavelength (j index). Furthermore, $\lambda(j) = 4600 \text{ Å} + j\,\delta\lambda$, where $\delta\lambda = 200$ Å, and the 11 weighting factors $w(j)$ defining the Johnson V filter are 0.01, 0.36, 0.91, 0.98, 0.80, 0.59, 0.39, 0.22, 0.09, 0.03, and 0.01 (Allen 1983).

We define our "standard model" for SS Cyg using the above parameters for the accretion disk, adopting $\dot{M}_T = 10^{-9} M_\odot \text{ yr}^{-1}$, and taking 100 radial grid points. A long run using these parameters gives the sequencing of outbursts LSSLSSLSS...,

where L stands for a long outburst and S denotes a short outburst. If we increase $\dot{M}_T$ to $1.5 \times 10^{-9}\ M_\odot\ \mathrm{yr}^{-1}$, we obtain the alternating sequence of long and short outbursts most commonly seen in SS Cyg. Osaki (1989) showed analytically using conservation of mass and angular momentum that, for typical model parameters (i.e., $\Sigma \propto r$ in quiescence and $\Sigma \propto r^{-3/4}$ in outburst), one expects about one-sixth of the stored matter in the disk to be accreted onto the WD during the course of an outburst. (This argument was generalized by Mineshige & Shields 1990 to include disks with arbitrary surface density profiles in outburst and quiescence.) The argument used by Osaki actually refers to an idealized situation in which the whole disk is in the high state and $\Sigma(r_{\mathrm{outer}}) = \Sigma_{\mathrm{min}}(r_{\mathrm{outer}})$ at $t = 0$, so that cooling starts immediately. By following the mass of the disk in our computations we find that, for the short outbursts, less than one-sixth of the disk is accreted (i.e., only about 3%), while in the long outbursts, more than one-sixth is accreted (about 30%). The difference between the two types of outbursts comes about because of differences in the disk mass at the time of onset of the instability. The outburst is triggered near the inner edge for both types of outbursts, and the heating front propagates to the outer edge, transforming the entire disk to the hot state. After the period of heating has ended, the surface density profile tries to readjust from the quiescent profile in which $\Sigma(r)$ increases with r, to a quasi–steady state profile in which $\Sigma(r)$ decreases with r. For outbursts which end up being "short," the disk mass and surface density at large radii are such that $\Sigma(r_{\mathrm{outer}})$ is less than $\Sigma_{\mathrm{min}}(r_{\mathrm{outer}})$. Hence, a cooling wave immediately begins to propagate back to smaller radii and to shut off the flow onto the WD. In addition, there is some mass very near the outer edge which does not heat to the high state. This cold matter does not partake of the general flow onto the WD—only a very small fraction of the entire disk accretes. For outbursts which end up being "long," the disk mass built up in quiescence is larger and the surface density near the outer edge is greater. The entire disk is ionized during the flat-topped part of the long outbursts because $\Sigma(r) > \Sigma_{\mathrm{min}}(r)$ even at the outer disk edge. Some amount of time must pass to allow enough accretion onto the WD so that $\Sigma(r_{\mathrm{outer}})$ can decrease to $\Sigma_{\mathrm{min}}(r_{\mathrm{outer}})$ and cooling can begin. It is this period of viscous decay in the high state which produces the flat-topped outbursts in SS Cyg. Once $\Sigma(r_{\mathrm{outer}}) = \Sigma_{\mathrm{min}}(r_{\mathrm{outer}})$, the cooling wave can begin to move inward and return the disk to its cool state. Significant accretion occurs during the viscous stage of the long outbursts, and more than one-sixth of what was present in the disk at the start of the outburst is accreted onto the WD during a long outburst. Cannizzo (1993) commented that the gas making up the disk mainly "sloshes back and forth" during a complete cycle of quiescence and outburst. This is not strictly true for the long outbursts; significant depletion of the disk does occur. As we will soon discover, however, a caveat which must temper this discussion concerns the number of radial grid points used in the model. As N increases, the fraction of the disk accreted—during both the long and short outbursts—decreases. The figures quoted earlier of 30% and 3% for the fraction of the quiescent disk accreted during the long and short outbursts, respectively, are for $N = 100$ points. The exact fractions of the disk which are accreted in the two types of outbursts may depend on other model specifics as well.

In Figure 2 we show the evolution of the surface density, midplane temperature, and effective temperature during the quiescent period between two consecutive bursts (Fig. 2*a*) following a long outburst and (Fig. 2*b*) following a short outburst. These are taken from a run in which long and short outbursts alternate—the "standard model" except $\dot{M}_T = 1.5 \times 10^{-9} M_\odot\ \mathrm{yr}^{-1}$. The solid curves show the 15 days of quiescent evolution (one curve per day), and the dotted curves show Σ_{max}, Σ_{min}, and $T_{\mathrm{max}} = T(\Sigma_{\mathrm{max}})$. (Recall that $T_{\mathrm{max}} < T_{\mathrm{min}}$.) The secondary mass transfer is producing the increase in Σ near the outer edge of the disk, and the viscous drift of material in the quiescent state shifts matter at small radii. For SS Cyg model parameters, both the long and short outbursts are always triggered near the inner edge of the disk by the viscous drift of matter in quiescence. By comparing Σ between Figures 2*a* and 2*b*, we see that the surface density at large radii is smaller after a long outburst has ended than it is after a short outburst has ended—more of the disk is accreted during a long outburst. The tendency for the surface density profile left over at the end of a long outburst to lead to the next outburst being a short one, and vice versa, was noted by Smak (1984). The density of lines in the Σ evolution makes it difficult to see the shift of matter at small radii. This is better seen in the evolution of T. The final T curve in both Figures 2*a* and 2*b* has almost reached T_{max} at the radius where the next outburst is triggered.

Figure 3 shows the evolution of Σ and T during the onset of a long outburst. (The evolution is very similar during the start of a short outburst.) The solid curves again show the disk evolution (0.1 day per curve), and the dotted curves show Σ_{max}, Σ_{min}, T_{min}, and T_{max}. The instability begins near the inner disk edge and propagates all the way to the outer edge, thereby heating the entire disk to the upper branch of the S-curve. As has been found in all previous studies, a narrow spike in Σ leads the heating front. The surface density at small radii begins to shift toward the $\sim r^{-3/4}$ outburst profile as more of the inner disk goes to the high state.

Figure 4 shows in detail how the cooling in the disk proceeds. For convenience, this experiment was started by placing the disk into a steady state (in the high state) with $\Sigma(r) = 0.95\Sigma_{\mathrm{min}}(r_{\mathrm{outer}})(r/r_{\mathrm{outer}})^{-3/4}$. The fact that $\Sigma(r_{\mathrm{outer}}) < \Sigma_{\mathrm{min}}(r_{\mathrm{outer}})$ ensures that cooling will start immediately. Figure 4*a* shows the evolution at the outer edge, and Figure 4*b* shows the evolution at the inner edge. The "stagnation" referred to above is evident in the pattern of cooling near the outer edge. The decrease in T is at first rapid once $\Sigma = \Sigma_{\mathrm{min}}$ in a given annulus, but it slows as T approaches the peak in the specific heat (i.e., $\sim 12{,}000$ K). Even after $T < T_{\mathrm{max}}$, it takes a long time to reach the lower stable branch of the S-curve. The cooling front spans a decreasing number of radial grid points as the front moves inward. Near the inner edge, the front comprises either one or no grid points. During most of its evolution the surface density of an annulus in the hot state just interior to the cooling front is being depleted by the outflow of matter. The thermal equation is not needed during these times because the inner disk is wholly on the upper branch of the S-curve and the outer disk is wholly on the lower branch. The cooling front formally exists only in the region between the two grid points separating the hot and cold regions. This fact enables us to save considerably on computing time. When Σ drops below Σ_{min} at one grid point, that annulus cools rapidly to the low state because stagnation is ineffective at small radii. (See also Figure 3 of Mineshige 1988.) This brief period of cooling is quite CPU intensive because the thermal equation (with its much smaller time step) must be calculated, and $t_{\mathrm{thermal}} \propto r^{3/2}$. Fortunately, the cooling lasts for a short fraction of the total time and so does not place a severe limitation on computer resources.

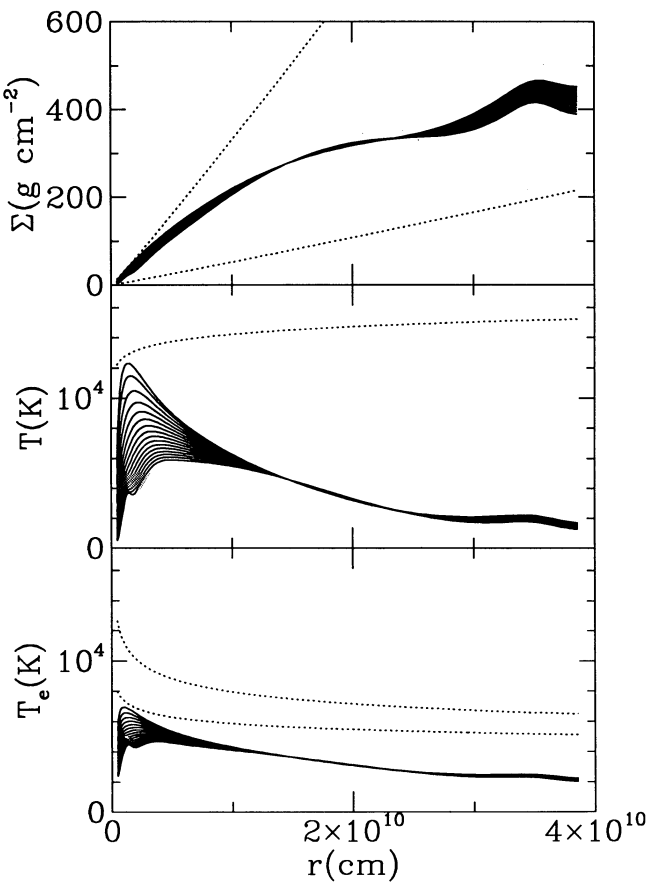

FIG. 2a

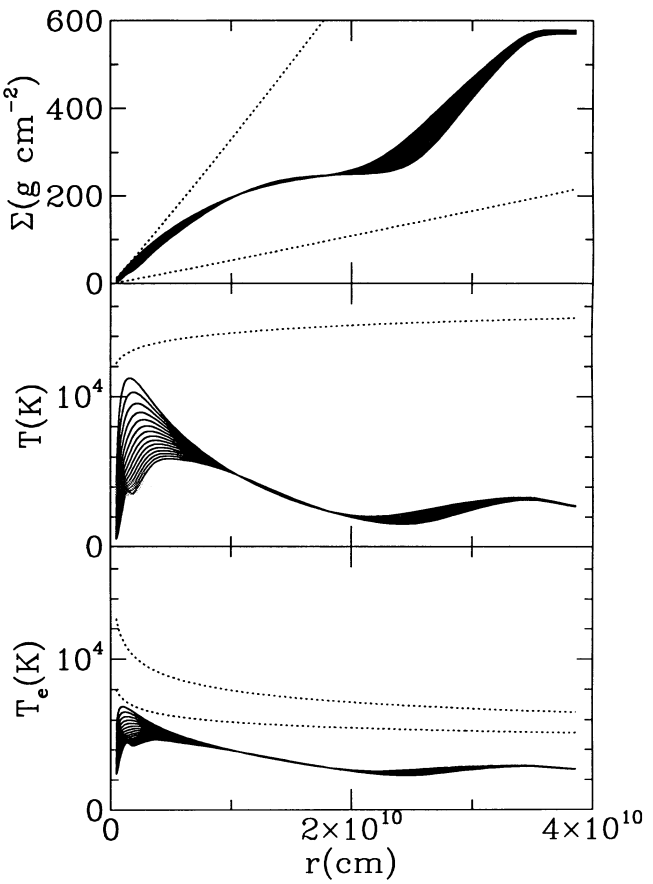

FIG. 2b

FIG. 2.—The evolution of the surface density Σ, midplane temperature T, and effective temperature T_e during the quiescent interval (*a*) following a long burst and preceding a short burst, and (*b*) following a short burst and preceding a long burst. The model assumes the "standard" input parameters given in the text. The separation between each of the curves is 1 day, and a total of 15 days of evolution is given in each run. The dotted lines show the physical conditions associated with Σ_{max} and Σ_{min}. The mass distribution shifts to smaller radii because of the viscous drift. The outbursts are always triggered near the inner disk edge for parameters appropriate to SS Cyg. The mass of the disk is greater during the quiescent period following the short outburst (note the higher surface density at large radii), and this causes the next outburst to have a "viscous plateau" during which time the entire disk is in the hot, totally ionized state.

3.2. *Dependence on Terms in Energy Equation*

In Figure 5 we see the effects of turning off different terms in the energy equation (eq. [2]). The changes that occur in each instance reveal something of the underlying physics. Setting the $P\,dV$ term to zero has a negligible effect—the PdV expansion of material represents only a small fraction of the energy budget. The advective term $v_r \partial T/\partial r$ is much more important. During the times of declining light from an outburst when the cooling front is traveling to smaller radii, there exists a strong decrease in temperature across the transition front (LPF). The matter which flows outward through this region from the hot side to the cool side of the front carries a great deal of heat with it, and thereby tends to slow the cooling front. When this term is turned off, the cooling front travels more quickly into the hot region, and sometimes the outflow of matter cannot proceed quickly enough to lower the surface density at radii just interior to the cooling front so that the velocity of the inward moving front and the velocity of the outflowing matter can come to equilibrium (see eqs. [3.10] and [3.11] of CSW). When this occurs, the cooling front is reflected outward as a heating front. This process can repeat several times until enough matter has accreted onto the WD so that the surface density is depleted to the extent that the cooling front can successfully propagate completely to the inner edge. This back-and-forth tendency of the transition fronts produces the "sawtooth" light curve in the third panel. In the fourth panel both the $P\,dV$ and advective terms are set to zero. The result is quite similar to that of the third panel. In the fifth panel, the $P\,dV$ and advective terms are turned back on, and the term which transports the radial heat flux $(3/2)c_p v(\Sigma/r)(\partial[r\,\partial T/\partial r]/\partial r)$ is set to zero. The radial heat flux is important during times when the heating front propagates from small to large radii during the onset of an outburst and transforms the disk to the high state. With this term turned off, the heating front cannot propagate completely to the outer edge for the short outbursts. Thus, the peak luminosities of the short outbursts are smaller, less matter is accreted onto the WD during the short outbursts, and more short outbursts must occur to build up to a long outburst. That the short and long outbursts seen in SS Cyg all rise to about the same peak brightness would argue that the heating front always goes nearly (or very nearly) to the outer edge of the disk. The types of deficiencies seen in the light curves in this figure can also be seen in the light curves of previous studies which neglected the advective or radial heat flux terms.

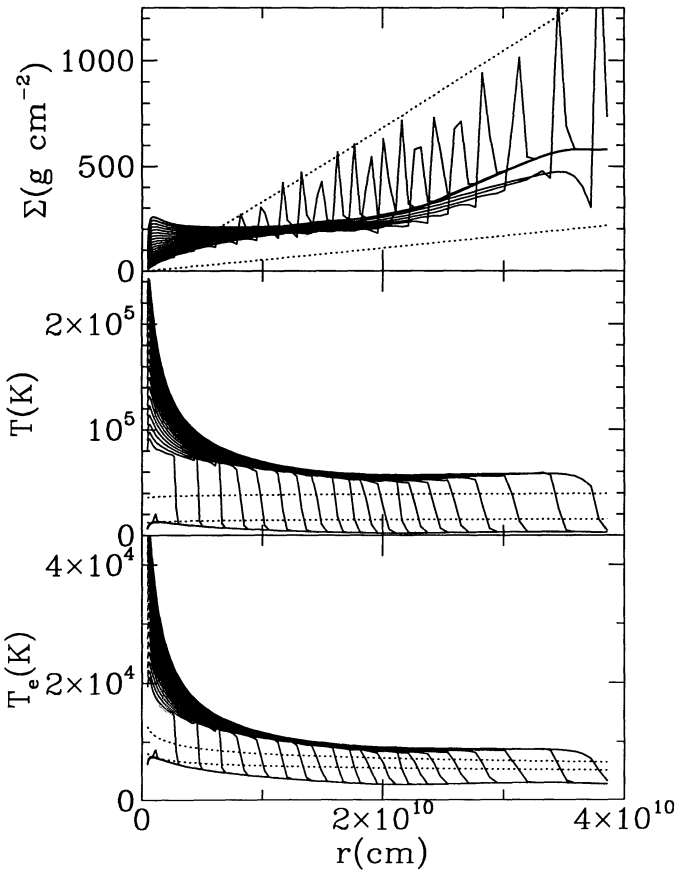

FIG. 3.—The evolution of Σ and T during the onset of a long outburst in the standard model. (The evolution is very similar during the onset of a short outburst.) The spike in Σ accompanies the heating pulse as it moves outward in the disk. Each curve is separated by 0.1 day, and the dotted curves show conditions associated with Σ_{max} and Σ_{min}.

3.3. *Dependence on Number of Grid Points*

The computations depicted in Figure 6*a*–6*e* show how changing the number of radial grid points N in the model affects the results. Fewer short outbursts occur in a given pattern for runs with larger N. The heating front which moves outward and transforms the disk to the hot state is communicated by a narrow spike in the surface density which is pushed outward by the high-viscosity material lying at smaller radii—the snowplow effect (LPF). When the grid points are closer together, the spike can be narrower and higher, and the front can propagate to larger radii where the difference between $\Sigma(r)$ and $\Sigma_{max}(r)$ is larger. With finer zoning, the fraction of the disk mass accreted during an outburst decreases because the length of time spent on the viscous plateau becomes shorter. This tendency is revealed in Figure 6*c* which shows the average duration of the long outbursts in each panel in Figure 6*a* (measured from $m_v = 11$). The rate of change in t_b with increasing N becomes small once N exceeds about 100. The speeds of the transition fronts are inversely related to their widths (CSW), and we underresolve the fronts until we have of order 100 grid points. LPF argue that a transition front cannot have a width less than about the disk thickness, or else the resulting radial pressure gradient would cause a departure from Keplerian flow which would increase the width of the front. Since $h/r \lesssim 0.01$ in quiescence, we should take $\gtrsim 100$ radial points to resolve the fronts adequately. All computations in this study except those shown in Figure 6 use 100 radial grid points. The amount of computer time required becomes very large for $N > 100$. All previous time-dependent studies of the disk instability process in dwarf novae have taken between about 20 and 40 radial grid points.

3.4. *Dependence on Inner Disk Radius*

Figure 7 shows the sensitivity of the computations to r_{inner}. The five panels show runs (*top to bottom*) using the standard model parameters, with $r_{inner}(\text{cm}) = 4.51 \times 10^8$ (100 grid points), 9.05×10^8 (95 grid points), 1.96×10^9 (87 grid points), 2.82×10^9 (82 grid points), and 3.84×10^9 (77 grid points). The grid point spacing is the same in these five models; we are merely eliminating grid points at the inner edge. The triggering of the outbursts is always near the inner disk edge in our computations; therefore, the inner disk radius strongly affects the recurrence time for outbursts t_c. Note that as r_{inner} increases, t_c increases and the number of short outbursts occurring between two long outbursts decreases. CSW showed that t_c is significantly shorter than the viscous drift time in quiescence measured from the outer disk edge. Their argument was somewhat misleading, however, because when t_c is governed by the viscous drift in quiescence as it is in these computations, it is associated with the drift at small radii, not at large radii.

3.5. *Dependence on Outer Disk Radius*

Figure 8 shows the sensity of the computations to r_{outer}. The five panels show runs (*top to bottom*) using the standard model parameters, with $r_{outer}(\text{cm}) = 3. \times 10^{10}$, 3.5×10^{10}, $4. \times 10^{10}$, 4.5×10^{10}, and $5. \times 10^{10}$. Each model has 100 grid points. The quiescent interval t_q increases slightly as r_{outer} increases, going from ~ 22 days (*top panel*) to ~ 25 days (*bottom panel*), where the crossing of $m_v = 11$ in the light curve has been used in defining the timescale. There is also an increase in t_b(S) and in t_b(L)—the durations of the short and long outbursts. These go from (*top to bottom*) ~ 6 days to ~ 13 days, and from (*top to bottom*) ~ 23 days to ~ 29 days, respectively. As regards sequencing, the number of short outbursts lying between two successive long outbursts increases as r_{outer} increases.

3.6. *Dependence on Variations in $\dot{M}_T$ and α*

In Figure 9 we show the effects of keeping α_{cold} and α_{hot} constant, and increasing the value of $\dot{M}_T$ by a factor of 4.5 over 2500 days. After the transient stage has ended, the sequencing of outbursts for the run is 2(LSSS)-2(LSS)-14(LS)-LSS-8(L). The sequencing of long and short outbursts changes in the sense that fewer short outbursts appear in a given pattern. We go from having three short outbursts between two long ones, to having purely long ones. We also see in this run a mild increase in the length of the long outbursts, while the length of the short outbursts remains constant. When $\dot{M}_T$ is larger, one builds up to the critical disk mass sufficient to support a long, viscous plateau-type outburst more frequently, and therefore there are fewer short outbursts between the long ones. Only a tiny fraction of the disk is accreted during a short outburst, whereas a much greater fraction is accreted during a long outburst. This can be seen in the panel showing the disk mass. The disk mass at the start of the long outbursts increases with time, whereas the disk mass at the end of the long outbursts is constant. The peak brightness of our model outbursts is somewhat fainter than that observed in SS Cyg; therefore, we use

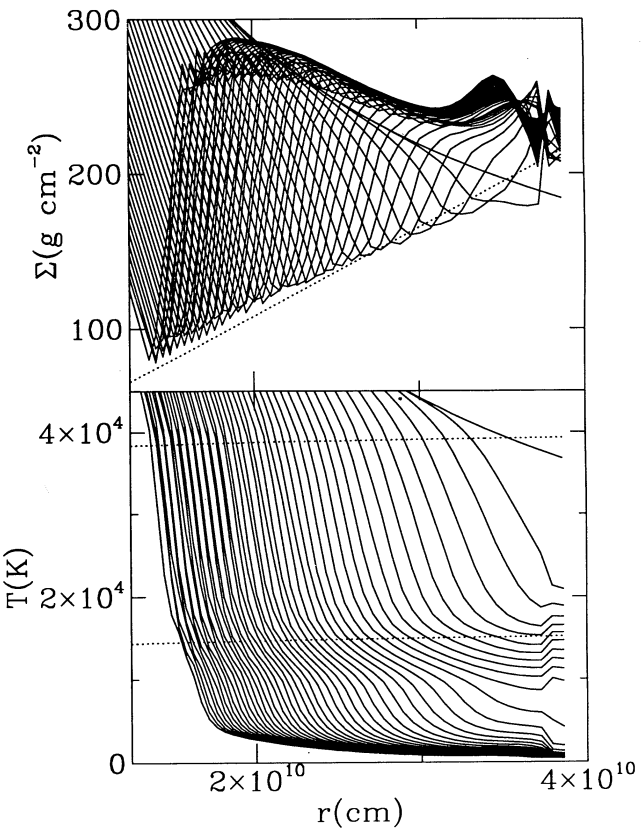

FIG. 4a

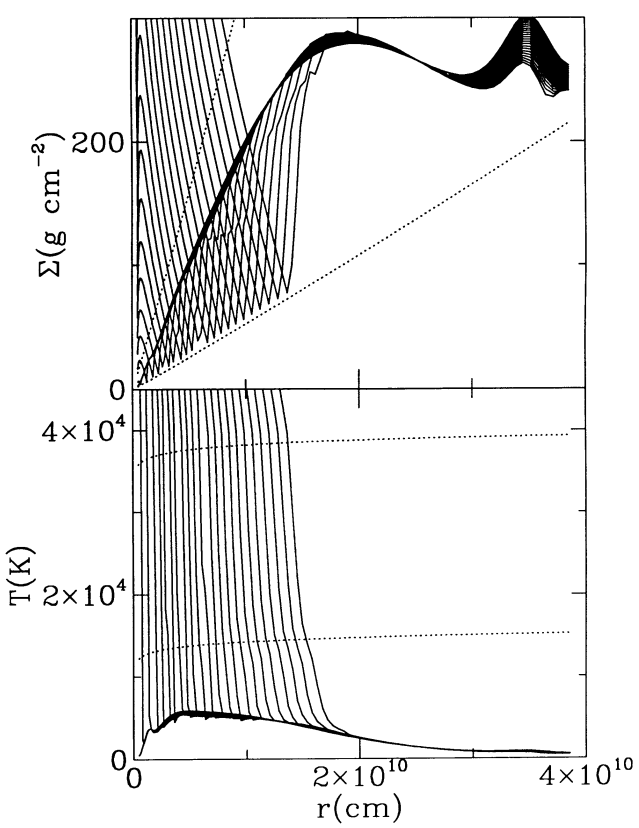

FIG. 4b

FIG. 4.—The response of the disk to a cooling transition front. We take standard model parameters, but rather than extracting this from a long sequence we initially adopt a steady state profile $\Sigma(r) \propto r^{-3/4}$, with $\Sigma(r_{outer}) = 0.95\Sigma_{min}(r_{outer})$. This ensures that cooling will begin immediately at the outer disk edge. (*a*) The first two panels show the evolution of Σ and T immediately after the run starts. Each line is separated by 0.1 day, and a total of 4.7 days of evolution is shown, including the $t = 0$ profile. The dotted lines show the physical conditions associated with Σ_{max} and Σ_{min}. One can see the "stagnation" associated with the enhanced specific heat near $\sim 10^4$ K by noting the pause in the cooling around $T = T_{max}$ at large radii. (*b*) The next two panels show the evolution of Σ and T following the evolution shown in (*a*). Each line is separated by 0.5 day, and a total of 11.5 days of evolution is shown. As can be seen by comparing $T(r, t)$ between (*a*) and (*b*), and as was originally noted by Mineshige (1988), stagnation is increasingly ineffective at smaller radii.

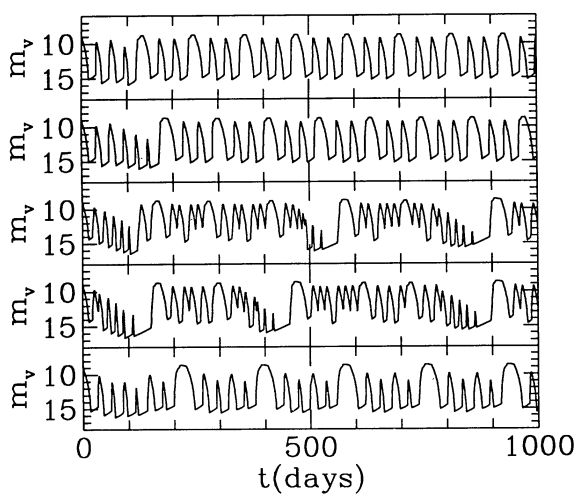

FIG. 5.—The effect of turning off different terms in the thermal energy equation (cf. eq. [2] in the text). The five light curves (*top to bottom*) are for computations in which we (1) use the full thermal equation, (2) set the "PdV" term to zero, (3) set the advective term to zero, (4) set both the PdV and advective terms to zero, and (5) set the radial energy flux term to zero.

the crossing of $m_v = 11$ in the light curve as our criterion for defining the quiescence interval t_q and outburst duration t_b rather than $m_v = 10$ as was done by CM (and most previous investigators) in studying the SS Cyg light curve. Since the triggering of outbursts is primarily a viscous process for SS Cyg parameters, there is virtually no change in t_q as $\dot{M}_T$ varies. All of the outbursts in this sequence—even the high $\dot{M}_T$ ones—are triggered at small radii in the disk.This may seem at odds with the results of DL which show that the recurrence time for outbursts t_c is independent of $\dot{M}_T$ for $\dot{M}_T$ small, but strongly dependent on $\dot{M}_T$ for $\dot{M}_T$ large. It is not clear why our model does not show this trend. Our α prescription is different, but this should not matter. DL implicitly assume $\alpha \propto r^{\epsilon}$, where ϵ is a few tenths. We do not assume a radial dependence of α on r. One might think that the reduction in α at small radii would endow a model with more of a propensity to have "outside-in" outbursts (which are triggered by Σ buildup from the secondary mass transfer) when $\dot{M}_T$ is large. Ichikawa & Osaki (1993) have recently shown, however, that both classes of models give bursts starting at small radii for low $\dot{M}_T$ and bursts starting at large radii for high $\dot{M}_T$. There may be some aspect of our input physics which predisposes our models to have inside-out outbursts.

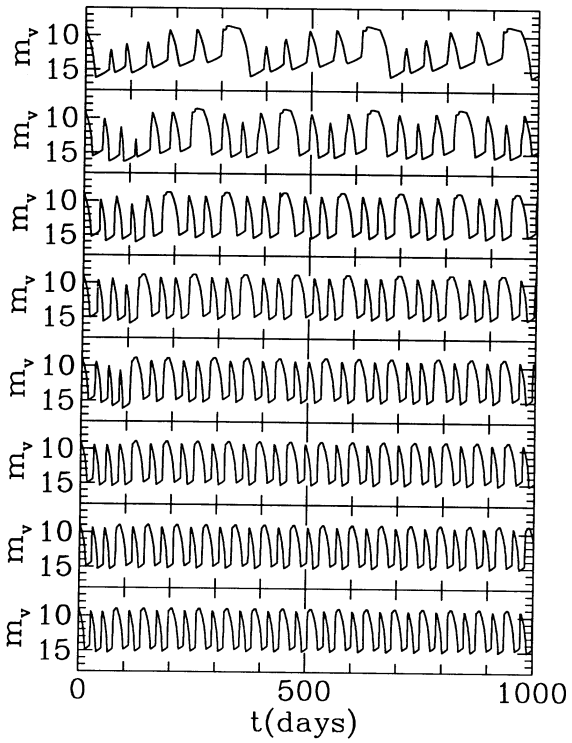

FIG. 6a

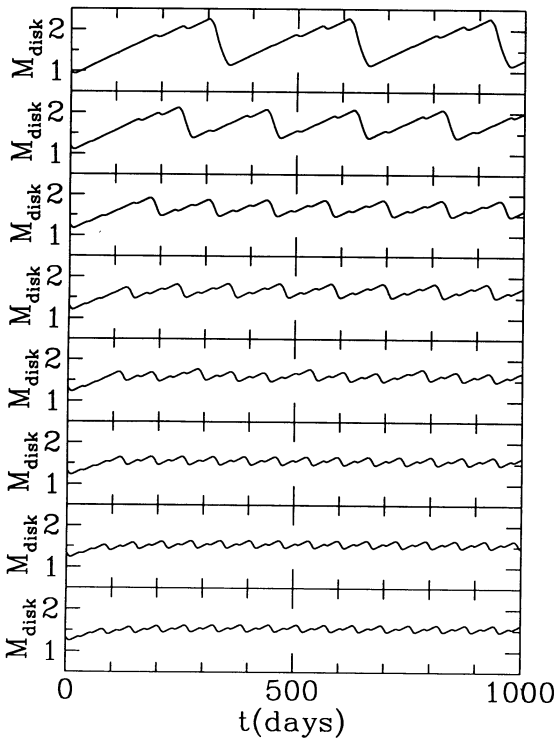

FIG. 6b

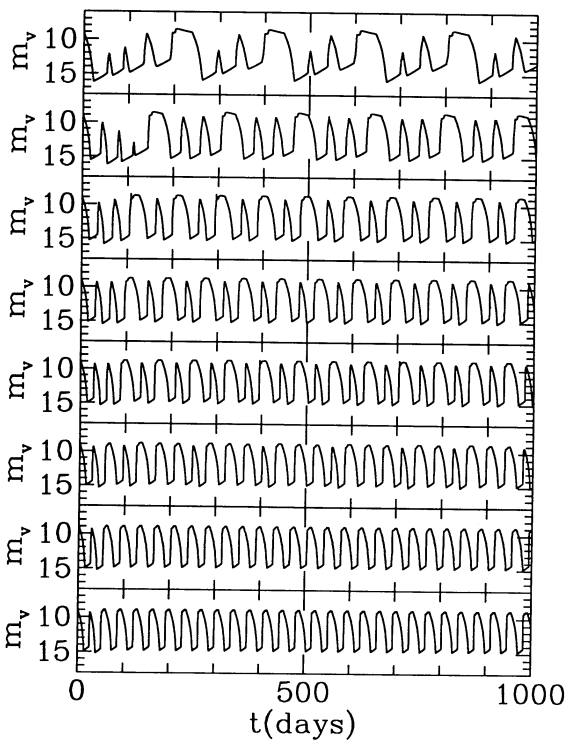

FIG. 6d

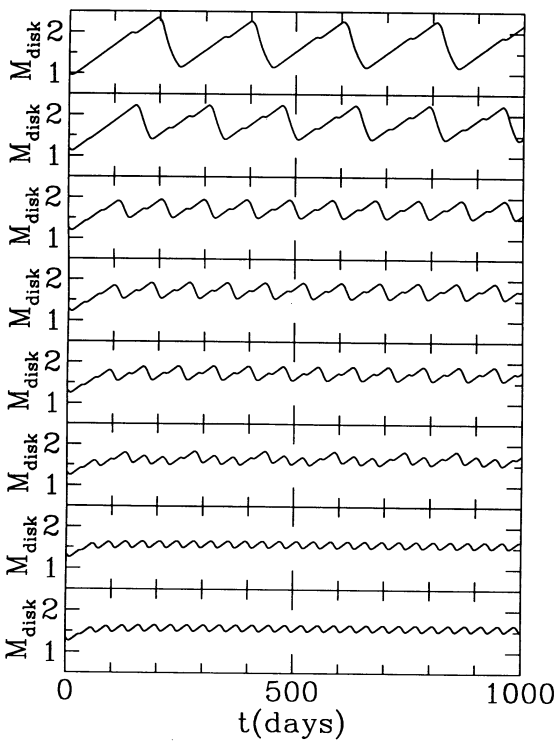

FIG. 6e

FIG. 6.—The effect of varying the number of grid points. The eight panels in each run (*top to bottom*) are for $N = 25, 50, 75, 100, 125, 150, 175, 200$. (*a*) The light curves for $\dot{M}_T = 1 \times 10^{-9} M_\odot$ yr^{-1}. (*b*) The disk mass (in units of 10^{24} g) for $\dot{M}_T = 1 \times 10^{-9} M_\odot$ yr^{-1}. (*c*) The average duration of the long outbursts in each panel of (*a*) (measured from $m_v = 11$). (*d*) The light curves for $\dot{M}_T = 1.5 \times 10^{-9} M_\odot$ yr^{-1}. (*e*) The disk mass (in units of 10^{24} g) for $\dot{M}_T = 1.5 \times 10^{-9} M_\odot$ yr^{-1}. The timescales associated with the outbursts become smaller as N increases.

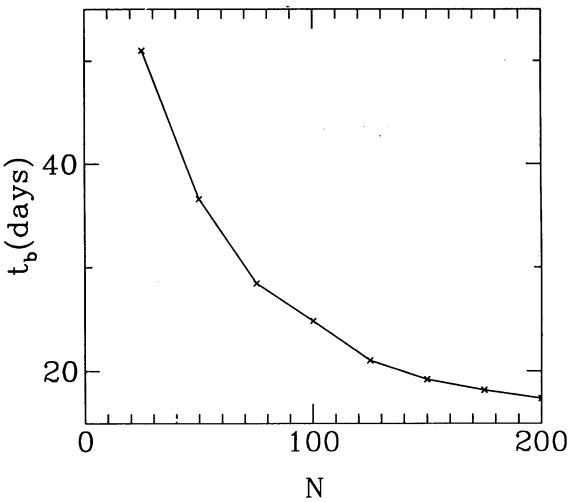

FIG. 6c

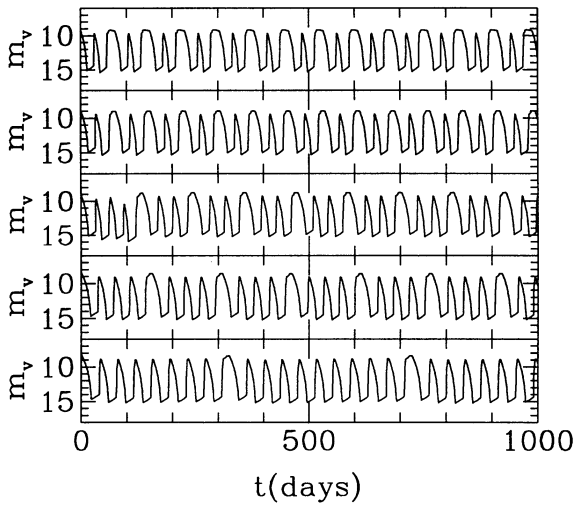

FIG. 8.—The effect of changing the outer radius of the disk. The input parameters are those from the standard model, and (*top to bottom*) we take r_{outer}(cm) = 3. × 10^{10}, 3.5 × 10^{10}, 4. × 10^{10}, 4.5 × 10^{10}, and 5. × 10^{10}. As r_{outer} increases, the number of short outbursts lying between two consecutive long outbursts increases. The burst timescales are relatively unaffected.

Figure 10 shows a run for which α_{cold} is increased by a factor of 2 over 2500 days, and $\dot{M}_T$ and α_{hot} are held constant. Increasing α_{cold} has the effect of (1) decreasing the critical surface density Σ_{max} which instigates heating and (2) decreasing the viscous drift time in quiescence. By increasing α_{cold} we also raise the amount of viscous dissipation in quiescence and thereby increase the flux emitted by the quiescent disk. After the initial transient, the sequencing of outbursts is 7(LS)-LSS-LS-11(LSS)-L. We basically go from having one short outburst in between two long ones, to having two. By decreasing Σ_{max}, we ensure a decrease in the mass of the disk at the onset of instability for the long outbursts. In the second panel in Figure 10, we see a secular decrease in the disk mass at the end of the quiescent intervals which precede long outbursts (except for a jump at the interface between LS and LSS behavior), while the mass at the start of the quiescent intervals which follow long outbursts remains constant. As the stored disk mass becomes progressively smaller, it becomes more difficult to produce a long outburst. At the start of the run, every other outburst is long; by the end of the run, every third outburst is long. As

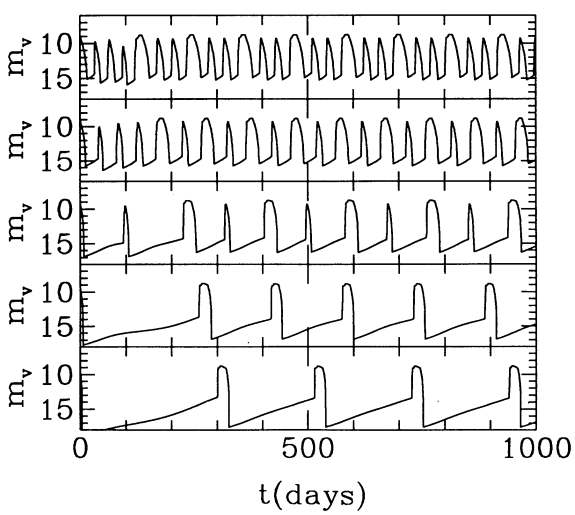

FIG. 7.—The effect of changing the inner radius of the disk. The input parameters are those from the standard model, and (*top to bottom*) we take r_{inner}(cm) = 4.51 × 10^8, 9.05 × 10^8, 1.96 × 10^9, 2.82 × 10^9, and 3.84 × 10^9. As r_{inner} increases, the recurrence time t_c increases, and the number of short outbursts lying between two consecutive long outbursts decreases.

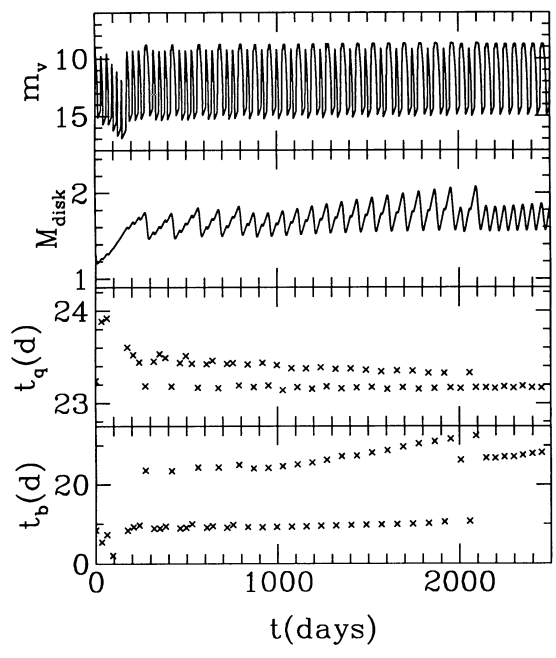

FIG. 9.—The effect of increasing $\dot{M}_T$ while keeping α_{cold} and α_{hot} constant. For this trial α_{cold} = 0.02, α_{hot} = 0.1, and $\dot{M}_T$ is increased at a linear rate from 0.5 × 10^{-9} $M_\odot$ yr^{-1} to 2.25 × 10^{-9} $M_\odot$ yr^{-1} during the 2500 days of the simulation. The four panels (*top to bottom*) show (1) the visual magnitude, (2) the disk mass (in units of 10^{24} g), (3) the quiescent interval between outbursts (measured between m_v = 11 on the descending and rising portions of the outbursts), and (4) the duration of the outbursts (also measured from m_v = 11). During the course of the run, the sequencing shifts to patterns which contain fewer short outbursts, while the recurrence and quiescent times remain nearly constant.

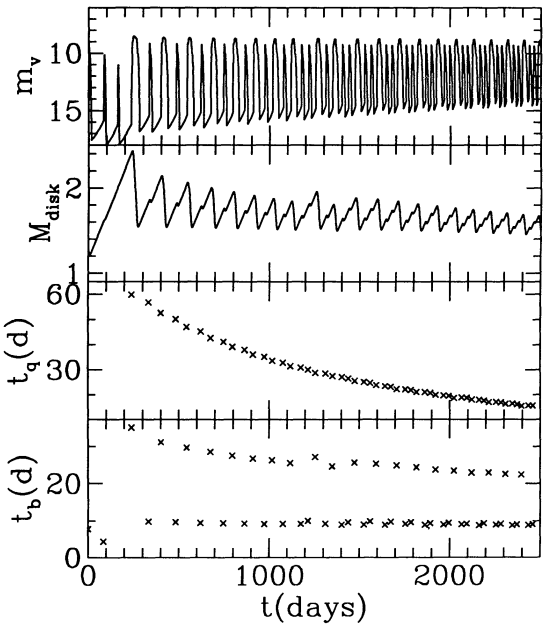

FIG. 10.—The effect of increasing α_{cold} while keeping α_{hot} and $\dot{M}_T$ constant. For this trial $\dot{M}_T = 1 \times 10^{-9}\ M_\odot\ \mathrm{yr}^{-1}$, $\alpha_{hot} = 0.1$, and α_{cold} is increased at a linear rate from 0.012 to 0.024 during the simulation. The quantities shown in each panel are the same as in Fig. 9 (*top to bottom*). The quiescent interval scales with the viscous drift time in quiescence and therefore becomes shorter as α_{cold} increases.

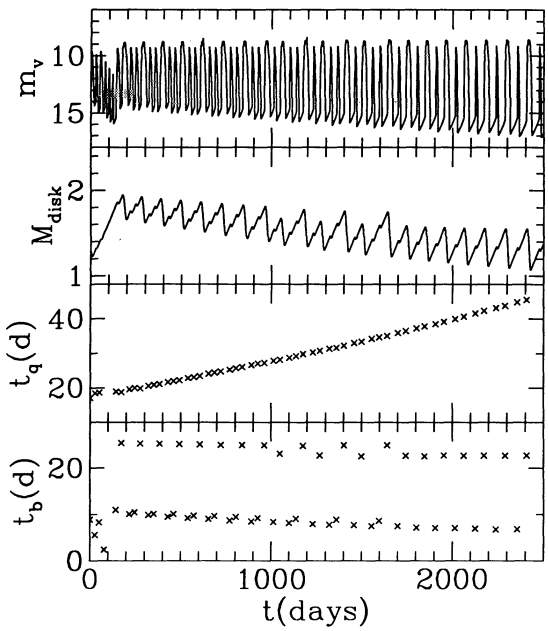

FIG. 11.—The effect of increasing α_{hot} while keeping α_{cold} and $\dot{M}_T$ constant. For this trial $\dot{M}_T = 1 \times 10^{-9}\ M_\odot\ \mathrm{yr}^{-1}$, $\alpha_{cold} = 0.02$, and α_{hot} is increased at a linear rate from 0.08 to 0.16 during the simulation. The quantities shown in each panel are the same as in Fig. 9 (*top to bottom*). The quiescent interval becomes longer as α_{hot} increases because of the reduction in Σ_{min}. This leads to a decreasing quiescent disk mass which also causes the quiescent disk to become fainter.

regards the time between outbursts, the decreasing quiescent viscous diffusion time is reflected in the decreasing quiescent intervals between outbursts. Finally, the outburst durations show only a small change. The short outbursts maintain a constant duration of about 9 days, whereas the long outbursts decrease from about 25 days to about 20. The duration of the long outbursts reflects how much mass the disk must lose before the cooling transition can begin—hence a decrease in the quiescent disk mass causes a decrease in t_b(long).

Figure 11 shows a run for which α_{hot} is increased by a factor of 2 over 2500 days, and $\dot{M}_T$ and α_{cold} are held constant. Increasing α_{hot} has the effect (1) decreasing the critical surface density Σ_{min} which instigates cooling and (2) decreasing the viscous drift time in outburst. We note in this run an increase in the quiescent interval between outbursts. After the initial transient evolution, the sequencing of outbursts is 7(LSS)-3(LS-LSS)-8(LS)—i.e., a progression from two short outbursts interspersed between two long outbursts, to a single short outburst. It might seem at first paradoxical that a change in a parameter associated with the high state of the disk could affect a quantity like t_q which depends on the viscous evolution time in the low state. Note, however, that the disk mass measured at the end of long outbursts decreases, while the mass at the start of long outbursts remains relatively constant (except for a jump which occurs in the transition region between the LSS and LS patterns.) This is just the opposite of what we saw in Figure 10. From Figure 4 which showed the evolution of $\Sigma(r, t)$ during the decay of an outburst, the Σ profile left behind by the cooling front traces the level of Σ_{min}. Therefore a decrease in Σ_{min} translates into a decrease in Σ at a given r after the cooling front has passed, and hence a smaller disk mass after the cooling front has run its course and the outburst has ended. We must rely on the viscous drift to skew the Σ distribution at small radii to trigger the next outburst, but since the surface densities at all radii are becoming smaller (with respect to Σ_{max}, which remains constant), it takes an ever greater fraction of the quiescent viscous drift time to move enough matter around in the disk to instigate the next outburst. Also, the decreasing quiescent disk mass leads to a fainter and fainter flux level from the quiescent disk. Finally, the durations of the outbursts decrease slightly—t_b(short) goes from about 10 days to about 7, and t_b(long) decreases in a step function from about 25 days (during the LSS sequences) to about 22 days (during the LS sequences).

Figure 12 shows a run for which both α_{hot} and α_{cold} are increased by a factor of 2 over 2500 days, and $\dot{M}_T$ is held constant. As we have just seen in Figures 10 and 11, changing either α_{hot} or α_{cold} separately produces opposite effects. This run is therefore interesting because it can show which parameter has the stronger influence. The sequencing hardly changes. After the transients have ended, we get 3(LS-LSS)-LSS-LS-16(LSS). Thus we are seeing basically LSS behavior. As regards t_q, the decrease in the quiescent viscous drift time from increasing α_{cold} beats out the effect of decreasing disk mass caused by increasing α_{hot}. This leads to a modest decrease in t_q. In the second panel we see that the disk mass both at the start and the end of long outbursts is decreasing—consistent with what we might have predicted given the results shown in Figures 10 and 11. The quiescent flux from the disk is essentially constant. The opposing tendencies brought about by varying the alphas together have very nearly cancelled out in this respect—i.e., the increasing viscous dissipation in quiescence brought about by increasing α_{cold}, and the decreasing quiescent disk mass brought about by increasing α_{hot}.

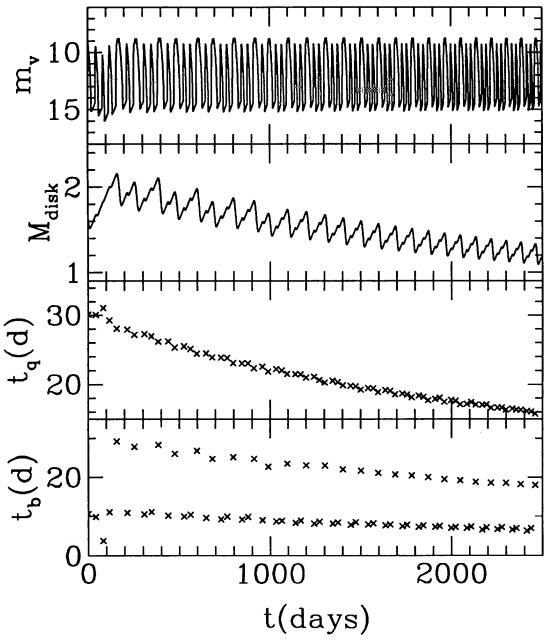

FIG. 12.—The effect of increasing both α_{hot} and α_{cold} at the same rate, while keeping $\dot{M}_T$ constant. For this trial $\dot{M}_T = 1 \times 10^{-9}\ M_\odot\ \mathrm{yr}^{-1}$, α_{cold} is increased linearly from 0.015 to 0.03, and α_{hot} is increased linearly from 0.075 to 0.15 during the simulation. The quantities shown in each panel are the same as in Fig. 9 (*top to bottom*). Although the changes in t_q caused by varying α_{cold} or α_{hot} separately are opposite, t_q is more sensitive to α_{cold} so that we decrease t_q during the run. There is only a slight change in the sequencing—we go from LS-LSS to pure LSS behavior—and the quiescent brightness level is virtually constant.

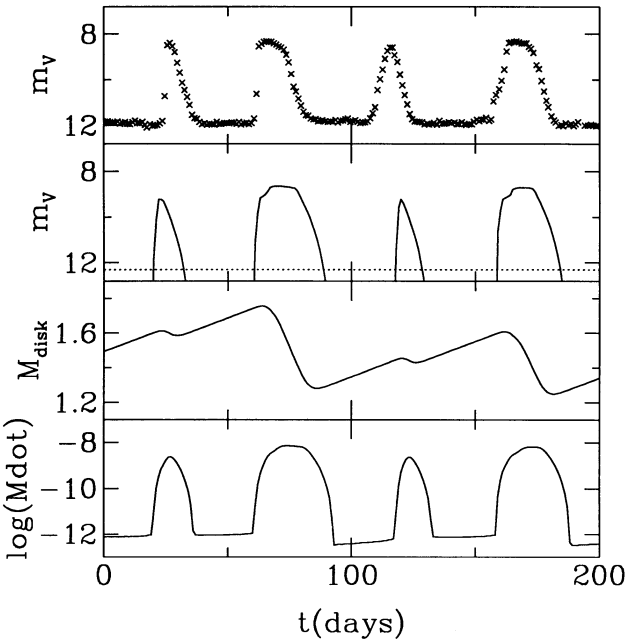

FIG. 13.—A comparison of observation and theory over a 200 day time interval. The panels (*top to bottom*) show (1) part of the AAVSO light curve of SS Cyg beginning at JD 2,447,000, (2) m_v taken from part of the run shown in Fig. 11 in which α_{hot} is being slowly varied, (3) the disk mass for (2) in units of 10^{24} g, and (4) the log of the rate of mass accretion from the inner disk onto the WD for (2) and (3) in $M_\odot\ \mathrm{yr}^{-1}$. The dotted line in the second panel shows the light level $m_v = 12.3$ expected for the K5/v dwarf in SS Cyg using our assumed distance of 100 pc and taking $M_v = +7.3$ (Allen 1983). This figure shows the long-short-long-short sequencing of outbursts which is observed most frequently in SS Cyg. In the model, $\dot{M}_T = 10^{-9}\ M_\odot\ \mathrm{yr}^{-1}$, $\alpha_{cold} = 0.02$, and α_{hot} increases linearly from 0.12288 to 0.12928 during the 200 days. The model light curve comes from t(days) = 1340 to 1540 of the run shown in Fig. 11.

Figure 13 shows the AAVSO light curve for a 200 day time span for SS Cyg which shows the typical long-short-long-short behavior in the sequencing. Also shown is a model light curve for a 200 day period, along with the mass of the accretion disk and rate of accretion onto the WD. For ease of viewing, we extract the model light curve from part of the run shown in Figure 11 during which the outburst recurrence time is about the same as that observed for this particular stretch in SS Cyg. The run is from t(days) = 1340 to 1540 in Figure 11, which means that α_{hot} is increasing uniformly from 0.12288 to 0.12928, $\alpha_{cold} = 0.02$, and $\dot{M}_T = 10^{-9}\ M_\odot\ \mathrm{yr}^{-1}$. There are some noticeable differences between the observed and theoretical light curves. Some of the observed rise times are slower than those we compute. This may indicate that our models should include more of the elements which lead to stagnation. As noted earlier, however, the complete stagnation effect as modeled by Mineshige (1988) is highly dependent on the exact assumed form of the $T(\Sigma)$ relation. This relation has been intentionally kept simple in our model. One can also see a slight pause near the onset of maximum light in the long (model) outbursts which is not seen in the observed outbursts. This appears to be an artifact of our brick wall outer boundary condition. When the surface density spike which precedes the heating front reaches the outer edge of the disk, it rams into the wall and transforms itself into an extremely thin and dense annulus for a short time. The ensuing radial gradients are very large and quickly cause this ring to spread out. It then merges back into the general disk flow. This "shoulder" at the beginning of the long outbursts is seen in other computations which adopt the brick wall outer boundary (e.g., LPF; see their Figs. 5*a* and *b*, Figs. 6*a* and *b*, and Figs. 7*a* and *b*). It would be more realistic to allow the outer edge to flex outward somewhat, as in the model of Ichikawa & Osaki (1992). This is a future improvement to be included in our model.

4. APPLICATION TO SS CYGNI

In the long-term light curve of SS Cyg one sees that there is a strong tendency for long and short outbursts to alternate. The most common behavior is that involving this simple alternation, and the second most common behavior consists of stretches during which two short outbursts lie between two long ones. The unit "LS" accounts for 38% of all outbursts, "LSS" makes up 29%, and "LSSS" comprises 8%. CM also found that there is a tendency for a given pattern to be stable for at least several repetitions before switching to a different mode. From the numerical experimentation of the previous section, we found that for our "standard model" we obtain a sequence in which two short outbursts lie between two long outbursts. With $\dot{M}_T$ increased to $1.5 \times 10^{-9}\ M_\odot\ \mathrm{yr}^{-1}$, we obtain an alternating sequence of long and short outbursts. We found, however, that the changes in the sequencing can also be produced by introducing changes in either α_{cold} or in α_{hot}, or by having the inner disk radius vary slightly. Can we use the long-term AAVSO light curve from SS Cyg to place constraints that might allow us to decide which of these four options is most likely?

CM noted an inverse relation in the long-term light curve of SS Cyg between the time-averaged values of t_c, the outburst

recurrence time, and the quiescent brightness of the system. By assuming that (1) the quiescent visual flux $f_v(q)$ has a contribution of about one-quarter from the bright spot, (2) fluctuations in the mass transfer rate from the secondary star $\dot{M}_T$ give rise to corresponding fluctuations in the bright spot flux, and (3) the luminosity of the secondary remains constant, CM inferred the existence of an inverse relation between $\langle t_c \rangle$ and $\langle \dot{M}_T \rangle$. By applying existing theory to their findings, CM came to the conclusion that variations in $\dot{M}_T$ were causing the long-term changes in SS Cyg. We note in Figure 9 a correlation between the ratio of the number of long outbursts $N(\mathrm{L})$ to the number of short outbursts $N(\mathrm{S})$ in a given time span and $\dot{M}_T$; therefore, we can check CM's finding in an independent way by going back to the data file containing the summary of outburst characteristics for SS Cyg and forming long-term moving averages of $N(\mathrm{L})/N(\mathrm{S})$. If CM's interpretation were correct in that $\langle t_c \rangle$ and $\langle \dot{M}_T \rangle$ are inversely related, then we should see an inverse relation between $\langle t_c \rangle$ and $\langle N(\mathrm{L})/N(\mathrm{S}) \rangle$.

In Figure 14 we show 1000 day moving averages for several quantities measured from the long-term AAVSO light curve of

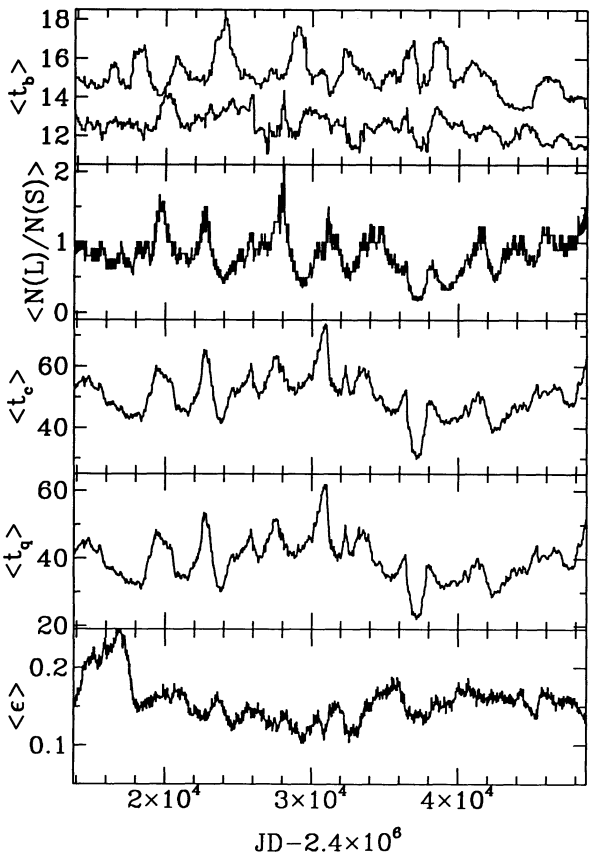

FIG. 14.—The moving 1000 day averages for the outburst properties associated with the complete AAVSO light curve of SS Cyg shown in CM. The five panels (*top to bottom*) show (1) the outburst duration time, measured from $m_v = 10$, and shown separately for the long and short outbursts; (2) the ratio of the number of long to short outbursts; (3) the recurrence time for outbursts (measured from $m_v = 10$ on the rising branch between consecutive outbursts); (4) the quiescent time between outbursts (measured from $m_v = 10$ between the declining portion of an outburst and the rising part of the next outburst); and (5) the fraction of time spent at brighter than 9th magnitude. For ease of viewing, the bottom curve in the first panel (showing the averaged value of t_b for the short outbursts) has been shifted upward by 5 days.

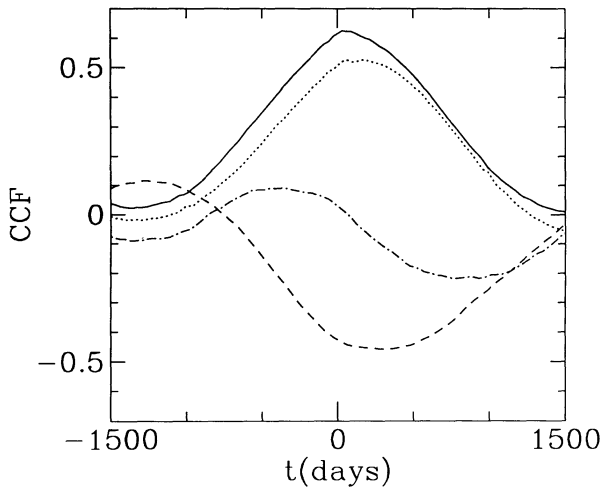

FIG. 15.—The cross-correlation functions between the moving averages of the various timescales associated with the outbursts, and $\langle N(\mathrm{L})/N(\mathrm{S}) \rangle$ (as shown in Fig. 14). *Solid curve*: for $\langle t_c \rangle$ with $\langle N(\mathrm{L})/N(\mathrm{S}) \rangle$; *dotted curve*: for $\langle t_q \rangle$ with $\langle N(\mathrm{L})/N(\mathrm{S}) \rangle$; *dashed curve*: for $\langle t_b(\mathrm{L}) \rangle$ with $\langle N(\mathrm{L})/N(\mathrm{S}) \rangle$; *dash-dotted curve*: for $\langle t_b(\mathrm{S}) \rangle$ with $\langle N(\mathrm{L})/N(\mathrm{S}) \rangle$.

SS Cygni. These parameters are the outburst duration t_b (shown separately for long and short outbursts), the ratio of the number of long to short outbursts $N(\mathrm{L})/N(\mathrm{S})$, the recurrence time t_c, the quiescent interval between outbursts t_q, and the fraction of time the system spends at brighter than $m_v = 9$. We see a striking correlation between the quantities plotted in the second, third, and fourth panels. Figure 15 shows the cross-correlation functions between the four timescales shown in Figure 14 and $\langle N(\mathrm{L})/N(\mathrm{S}) \rangle$. The recurrence and quiescent times are directly correlated with the ratio of number of long to short outbursts, the outburst duration for long outbursts is inversely correlated with $\langle N(\mathrm{L})/N(\mathrm{S}) \rangle$, and the outburst duration for short outbursts shows no correlation. If changes in $\dot{M}_T$ were causing the fluctuations in $\langle N(\mathrm{L})/N(\mathrm{S}) \rangle$, and if $\langle \dot{M}_T \rangle$ was varying inversely with $\langle t_c \rangle$, we should see an inverse correlation between $\langle N(\mathrm{L})/N(\mathrm{S}) \rangle$ and $\langle t_c \rangle$ (or between $\langle N(\mathrm{L})/N(\mathrm{S}) \rangle$ and $\langle t_q \rangle$) instead of the observed direct correlation. As noted earlier, in our model, outbursts are triggered at small radii, and hence there is no dependence of recurrence time on mass transfer rate. The key question is as follows: Would the change in sequencing shown in Figure 9 still hold if there were a transition from inside-out to outside-in outbursts at some point for a model in which $\dot{M}_T$ were gradually increased? That is, would there still be a progressive diminution in the number of short outbursts lying between two successive long ones? The results of Ichikawa & Osaki (1993; see their Fig. 2) would indicate that this trend *is* robust. The reduction in the number of short outbursts is evident in their model with $\alpha_{\mathrm{cold}} \propto r^{0.3}$ for the outside-in outbursts. This makes sense when one considers that the only difference between the long and short outbursts is the disk mass at the onset of an outburst.

CM criticized the finding of Hempelmann & Kurths (1990, hereafter HK90) of an inverse t_c-$\dot{M}_T$ relation because HK90 had used all the points in the AAVSO light curve (both quiescent and outburst values) in obtaining their estimate of $\dot{M}_T$. CM in turn also found an inverse t_c-$\dot{M}_T$ relation by restricting their attention to just the quiescent values of m_v, and assuming that bright spot fluctuations lead to quiescent light fluctuations. It

now appears that this was also wrong. More recently, Hempelmann & Kurths (1993) have noted the difficulty in using the light curve to infer relative changes in $\dot{M}_T$. Whether one obtains an inverse relation or a direct relation between $\dot{M}_T$ and t_c depends on such factors as the detailed shape of the rise and decay of the outbursts. In addition, our modeling has shown that the disk is not in steady state during the rise and decay portions—thus we are sampling both steady state and non–steady state behavior at different parts of the light curve. By comparing the last three panels of Figure 13 with each other, we see how one might at least obtain a crude estimate of a long-term moving average of $\dot{M}_T$. The only time during which steady state accretion onto the WD occurs is on the flat-topped part of the long outbursts. Assuming that all the mass which leaves the secondary ultimately accretes onto the WD, and that the rate of accretion within the disk is fairly constant when one is on a viscous plateau (which seems to be supported by the $\dot{M}_{\rm disk}$ values in the fourth panel of Fig. 13), one might hope to get a reasonable estimate of the averaged mass transfer by considering the moving average of the fraction of the time ϵ that SS Cyg spends on the flat-topped portion of the long outbursts. We show this quantity in the fifth panel of Figure 14, where $m_v = 9$ has been taken as our dividing line. There are no obvious relations between fluctuations in $\langle\epsilon\rangle$ and those in the other quantities. Aside from the time before JD 2,420,000 (which may be unreliable due to the small number of observations per daily mean), the fluctuations in $\langle\dot{M}_T\rangle$ would appear to be small—$\sim$20%–30%. Although this estimator of $\langle\dot{M}_T\rangle$ is admittedly crude, there is no obvious relation between fluctuations in this parameter and $\langle t_c\rangle$ to confirm the earlier findings of HK90 or CM.

Let us consider next variations in α. Figures 10 and 11 show how variations in $\alpha_{\rm cold}$ and $\alpha_{\rm hot}$ affect the sequencing. For $\dot{M}_T$ constant, increasing $\alpha_{\rm cold}$ increases the frequency of short outbursts and decreases t_q (and t_c), while increasing $\alpha_{\rm hot}$ decreases the frequency of short outbursts and increases t_q (and t_c). Either one of these two possibilities is therefore viable. It is interesting to note that, were $\alpha_{\rm cold}$ and $\alpha_{\rm hot}$ to vary together, the opposing effects they each produce separately would cancel as far as changes in the sequencing of long and short outbursts and variations in the level of flux from the quiescent disk are concerned. The recurrence time is more sensitively dependent on $\alpha_{\rm cold}$ than $\alpha_{\rm hot}$, so t_c and t_q would still vary. It would appear, therefore, that the α fluctuations must be independent of each other—i.e., either (1) $\alpha_{\rm cold}$ remains constant and $\alpha_{\rm hot}$ varies, or (2) $\alpha_{\rm hot}$ remains constant and $\alpha_{\rm cold}$ varies. The second option may be somewhat less likely because, when $\alpha_{\rm cold}$ varies, there is a positive correlation between t_b(L) and N(L)/N(S) (see Fig. 10), rather than the inverse correlation evident in the data in Figures 14 and 15.

Finally, we consider variations in $r_{\rm inner}$. If $r_{\rm inner}$ were to vary with time, this would lead to changes in t_c and N(L)/N(S) as shown in Figure 7. Some workers have presented arguments that SS Cyg may be a weak intermediate polar, so that a magnetic field from the WD disrupts the inner edge of the accretion disk (see, e.g., Giovannelli & Martinez-Pais 1991). For example, if the soft X-ray pulsations (SXPs) in SS Cyg arise at the interface between the boundary layer and accretion disk, then the variations between 7.4 s and 10.4 s seen in the period associated with the SXPs could indicate that $r_{\rm inner}$ is varying (Jones & Watson 1992). The sense of the changes in t_c and N(L)/N(S) seen in Figure 7 (as $r_{\rm inner}$ is made to increase) agrees with that seen in SS Cyg in that longer recurrence times accompany larger values of N(L)/N(S).

We have seen that if one were to appeal solely to variations in $\dot{M}_T$ to explain the fluctuations seen in SS Cyg, one would not be able to account for the large variations seen in t_q (and t_c). Since the outbursts begin at small radii in the accretion disk in our model, the quiescence and recurrence timescales depend solely on viscous processes and are thus independent of the mass transfer. This is evident in the third panel of Figure 9. A further problem lies in the variations in the quiescent flux. CM found an inverse relation between t_c and quiescent flux in SS Cyg (see their Fig. 15). If variations in $\langle\dot{M}_T\rangle$ were causing the long-term fluctuations, and if our model had input physics such that $\langle\dot{M}_T\rangle$ were inversely related to $\langle t_c\rangle$ as in DL, then $\langle\dot{M}_T\rangle$ would have to be anticorrelated with the quiescent flux $f_v(q)$ to account for the inverse correlation between t_c and $f_v(q)$. Variations in either $\alpha_{\rm cold}$ or $\alpha_{\rm hot}$ can better account for the sense of the observed fluctuations in $f_v(q)$. We see in Figure 10 that as $\alpha_{\rm cold}$ is increased, the level of the quiescent flux arising from the accretion disk goes up due to the increased viscous dissipation. Thus (1) more short outbursts correspond to (2) shorter recurrence times and (3) a higher quiescent flux, all as observed in SS Cyg. Similarly, from Figure 11 we see that as $\alpha_{\rm hot}$ is increased, (1) the quiescent disk flux decreases (because the disk mass in quiescence decreases), (2) the recurrence times increase, and (3) the fraction of short outbursts drops. These variations again all go in the same sense as the observed ones. If this scenario is right and either $\alpha_{\rm cold}$ or $\alpha_{\rm hot}$ is varying, while $\dot{M}_T$ is relatively constant, then the changes in $f_v(q)$ would not be caused by variations in the bright spot flux as assumed by CM. The variations seen in quiescence would reflect changes in the flux level from the disk itself. In Figure 7 we see that the quiescent disk just after an outburst has ended becomes fainter as $r_{\rm inner}$, t_c, and N(L)/N(S) increase, so variations in $r_{\rm inner}$ would also work. The amplitude of the dwarf nova outbursts seen in SS Cyg is about 3.3–3.5 mag; the amplitudes we compute are larger—about 6–7 mag. Whereas the light emitted by SS Cyg in outburst comes primarily from the accretion disk, the light in quiescence has contributions from the secondary star, bright spot, WD, and possibly heating effects on the accretion disk atmosphere having to do with interactions between the WD and inner disk edge. It is not unreasonable to expect that, by considering solely the disk luminosity, we overestimate the amplitude of the outbursts. In Figures 10 and 11 we saw that changes of a factor of 2 in either $\alpha_{\rm cold}$ or $\alpha_{\rm hot}$ lead to changes in the quiescent flux from the disk of about 3 mag. If we were to include in our light curves a steady light level corresponding to the flux from the secondary star and bright spot, e.g., the fluctuations in quiescent light coming from the disk would be much smaller and could account for those observed. (The long-term fluctuations of the quiescent magnitude in SS Cyg have an amplitude of a few tenths of a magnitude [CM].) Finally, it is also possible that uncorrelated changes in $\dot{M}_T$ and α may be occurring simultaneously. Although the $\dot{M}_T$ changes would not affect the burst recurrence times, they would have to be small enough so as not to swamp the changes in $\langle N$(L)/N(S)$\rangle$ caused by the α fluctuations.

5. DISCUSSION

The results of our numerical experiments are somewhat unexpected. CM had formed what seemed to be a self-consistent picture between the previously existing theory (from CSW and DL) and the long-term variations in SS Cyg. In particular, theory predicts the inverse $\langle t_c\rangle$–$\langle\dot{M}_T\rangle$ relation for systems in which the mass transfer rate is large. The one loose thread had been the fact that the outbursts in SS Cyg show the

alternating long-short pattern. Now we have shown that if fluctuations in $N(\mathrm{L})/N(\mathrm{S})$ were indeed caused by fluctuations in $\langle \dot{M}_T \rangle$, then $\dot{M}_T$ and t_c would have to be directly related, rather than inversely related as previous theory would have predicted. Cannizzo (1993) noted that it would be a challenge to disk modelers to be able to reproduce the long-short-long-short sequencing and yet also obtain the inverse $\langle t_c \rangle$—$\langle \dot{M}_T \rangle$ relation, because the former were thought to be produced by "inside-out" bursts, while the latter feature is associated with "outside-in" bursts. Ichikawa & Osaki (1993) have recently shown, however, that long-short-long-short sequencing occurs independently of where the outbursts originate. It now seems that fluctuations in $\langle \dot{M}_T \rangle$ would not be able to explain the observed long-term fluctuations in the sense postulated by HK90 and CM, and that the long-term changes in the quiescent brightness of SS Cyg which CM took to be evidence of mass transfer fluctuations are actually caused by changes in the level of brightness of the accretion disk itself. These changes can be brought about by introducing slow variations in either α_{hot} or α_{cold}—but both cannot be varying in unison or the quiescent light from the disk would be constant.

Variations in r_{inner} are also capable of providing the right sense of change in t_c, $N(\mathrm{L})/N(\mathrm{S})$, and $f_v(q)$. The strength of the dependence of t_c on $N(\mathrm{L})/N(\mathrm{S})$ in Figure 7 is stronger, however, than that observed in SS Cyg. In the first panel of Figure 7 where we adopt $r_{\mathrm{inner}} = 5 \times 10^8$ cm, the sequencing is LSS and t_c is about 40 days, roughly in agreement with that observed in SS Cyg. In the second and third panels where the LS sequencing is occurring, t_c is about 50 and 100 days, respectively, and in the fourth and fifth we have only long outbursts, and t_c is about 150 and 250 days, respectively—much longer than in SS Cyg. Also, the timescales associated with the inner disk are very short compared to the timescales of the fluctuations in the long-term light curve. If the radius of the boundary layer/accretion disk interface were varying in some manner due to changes in the magnetic field of the WD, these changes would have to be capable of producing cumulative variations that were stable on timescales of years. On the other hand, earlier workers have shown evidence that SS Cyg has a disrupted inner disk due to a magnetic field on the WD, so we must seriously consider the possibility that $r_{\mathrm{inner}} \neq r_{\mathrm{WD}}$. Fabbiano et al. (1981) argue in favor of intermediate polar status for SS Cyg on the basis of a similarity in optical/UV/X-ray spectra between AM Her and SS Cyg at minimum light. Ghosh & Lamb (1977, 1979a, b) presented a magnetohydrodynamical theory of the interaction between the magnetic field from the accreting star and the inner edge of the accretion disk, and in their theory the inner disk radius (the "standoff radius" at which gas and magnetic pressures balance) varies as $\dot{M}(r_{\mathrm{inner}})^{-2/7}$. In Figure 13 we see that, in the disk instability model, the rate of accretion at the inner disk edge varies by about four orders of magnitude in going from quiescence to outburst. (This result must be tempered, however, by the possibility of evaporative wind processes occurring in the inner disk [Cannizzo & Pudritz 1988; Meyer 1991; Vitello & Shlosman 1993]). One possible scenario is that, in the high state, the rate of accretion at the inner edge is great enough so that $r_{\mathrm{inner}} \simeq r_{\mathrm{WD}}$, but that in the low state r_{inner} exceeds r_{WD} by some nominal factor. The r_{inner} used in our computations would then represent some average over the low and high states. If there were some long term changes in the strength of the magnetic field from the WD, minor variations in $\langle r_{\mathrm{inner}} \rangle$ could be responsible for changes from LS to LSS, while other mechanisms might play a role in producing sequences for which $N(\mathrm{L})/N(\mathrm{S}) > 1$. If secular changes in r_{inner} only were required to provide the ability for the sequencing to transition from LS to LSS, then the long recurrence times in the last three panels of Figure 7 would not be a problem.

One of the major changes in going from CM to the present study is the realization that, within the disk instability picture, long-term variations in $f_v(q)$ seen in SS Cyg are more likely to be due to changes in the brightness level of the disk than the bright spot. Hassall, Pringle, & Verbunt (1985) pointed out a potential problem, however, with the disk instability model in this regard. These authors show that the UV level from WX Hyi decreases during the quiescence interval, and they noted that in the disk instability model it always increases. More recently, Szkody et al. (1991) show that long-period systems tend to have decreasing UV fluxes during quiescence, whereas short-period systems have flat or increasing fluxes. It is important to distinguish here between short- and long-term changes in the disk flux. Disk modelers have argued that, since the quiescent disk is so faint compared to the secondary star, WD, and bright spot, the UV flux seen during quiescence is unlikely to come from the disk. It may reflect the cooling of the white dwarf, or some process associated with the evaporation of the inner disk (e.g., Pringle 1988; Meyer 1991; Cannizzo 1993). The very long term changes in $f_v(q)$ which are of interest in this study are much smaller than the factor of ~ 2 UV decreases seen between outbursts in dwarf novae (e.g., Fig. 3 of Hassall et al. 1985). Figure 15 of CM shows the long-term changes in $m_v(q)$ in SS Cyg to be $\lesssim 0.1$ mag. As noted at the end of the last section, the actual long term changes in $m_v(q)$ from the disk which we saw in Figures 10 and 11 are several magnitudes, but when viewed simultaneously with a much brighter source, they would amount to only ~ 0.1 mag.

It appears unlikely that secular variations in $\dot{M}_T$ can bring about the large fluctuations in the recurrence times seen in SS Cyg. For the reasons given above, it seems more likely that changes in either α_{hot} or α_{cold} would be responsible. Since the fluctuations in $f_v(q)$ and $N(\mathrm{L})/N(\mathrm{S})$ produced by changing α_{cold} go in the opposite sense from those produced by changing α_{hot}, it would appear that α_{cold} and α_{hot} could not be varying in step with each other and by the same factor. (Exact cancellation of variations in t_q does not occur because the dependence of t_q on α_{cold} is stronger than that on α_{hot}.) For instance, one could not take $\alpha = \alpha_0(h/r)^n$, for example, and have α_0 be a slowly varying function of time. Also, the timescales for the fluctuations seen in the quantities plotted in Figure 14 are long—5–10 yr. That all timescales associated with the disk are so much shorter than this would argue against the disk as being the origin of these fluctuations. Could it be that either α_{cold} or α_{hot} is influenced by $\dot{M}_T$, and that slow changes in $\dot{M}_T$ are brought about by magnetic cycles in the secondary star? If this were true, to account for the sense of the various correlations in Figure 14, one could either have α_{cold} being an inverse function of $\dot{M}_T$ while α_{hot} remains constant, or else have α_{hot} be directly proportional to some power of $\dot{M}_T$ while α_{cold} remains constant. Neither of these options is appealing. One would qualitatively expect for the strength of α_{cold} to vary directly as $\dot{M}_T$ (if it is indeed mediated in some way by $\dot{M}_T$), not inversely. Furthermore, if the disk were affected by the strength of the mass stream impact, it would make more sense if both α_{cold} and α_{hot} varied, or at least that α_{cold} had a stronger dependence, since the disk spends about 3 times as much time in quiescence as in outburst in SS Cyg. In the picture of Vishniac & Diamond (1989, 1992),

for instance, internal waves excited by the impact of the mass stream from the secondary on the outer edge of the accretion disk provide the viscous dissipation and transport angular momentum. Strong support for a model of the type advocated by Vishniac & Diamond (in which the viscosity is a function of $\dot{M}_T$) is provided by the so-called VY Scl stars. These are thought to be novalike systems in which the mass transfer sometimes shuts off. The brightness of these systems often decreases by several magnitudes, and remains at a faint level for an extended period before returning to the high state (Rosino, Romano, & Marziani 1993). Computations using the disk instability model show that it is very difficult to reproduce this behavior if α remains constant when the mass transfer is shut off (Honeycutt, Cannizzo, & Robertson 1993). There is a strong tendency for outbursts to continue long after the mass transfer ceases due to the triggering of the instability at small radii. If $\alpha_{\rm cold}$ were to become small along with $\dot{M}_T$, however, this would elevate $\Sigma_{\rm max}$ and also increase the viscous diffusion time in quiescence, thereby preventing outbursts. Unfortunately, as mentioned earlier, our requirement on the $\alpha_{\rm cold}(\dot{M}_T)$ relation, if it is to account for the sense of the long-term variations seen in SS Cyg, is that it be an inverse relation rather than a direct relation. (This would be for the scenario in which $\alpha_{\rm cold}$ varies and $\alpha_{\rm hot}$ is constant.)

What about a causal relationship between $\langle \dot{M}_T \rangle$ and $\langle r_{\rm inner} \rangle$? As noted earlier, the Ghosh & Lamb theory predicts a mild inverse dependence of $r_{\rm inner}$ upon $\dot{M}(r_{\rm inner})$. One might imagine that, over very long timescales, the mean rate of accretion at the inner edge of the disk depends on the mass of the accretion disk. During periods when the rate of mass transfer is high, the disk mass would be greater, on average, and the mean inner disk radius would be smaller. One possible drawback of this idea is that it may require rather large variations in $\langle \dot{M}_T \rangle$ to affect significantly $r_{\rm inner}$. Also, the fluctuations shown in the last panel of Figure 14 of $\langle \epsilon \rangle$, our indicator for $\langle \dot{M}_T \rangle$, do not show any obvious correlation with the fluctuations in $\langle N(\mathrm{L})/N(\mathrm{S}) \rangle$ or $\langle t_c \rangle$.

It is not necessary to invoke changes in $\dot{M}_T$. It seems logical to use the secondary star to power long-term fluctuations since the secondary is the only object in a CV which is capable of providing changes on such long timescales, but maybe some agent other than the mass stream which carries information about the physical state of the secondary star could influence the disk. What if the magnetic field from the secondary threaded the outer part of the accretion disk, and slow changes in the strength of the field were to have an effect on the α's? In this scenario, it may be more probable that $\alpha_{\rm hot}$ is some "universal constant" (Tout & Pringle 1992) and that $\alpha_{\rm cold}$ is what varies on a long timescale. Figure 16 shows the ratio of the electron pressure (supplied by free electrons) to total pressure as a function of temperature. In the low state ($T \lesssim 10^4$ K), the number of free electrons is a steep function of the temperature, while in the high state ($T \gtrsim 10^{4.5}$ K), the disk is uniformly ionized. The currently favored model for providing the viscous dissipation involves the shear amplification of a toroidal magnetic field (Balbus & Hawley 1991), coupled with the Parker instability (Tout & Pringle 1992). The fact that $\alpha_{\rm hot} > \alpha_{\rm cold}$ may be a consequence of the higher degree of ionization of the gas in outburst versus quiescence (i.e., total vs. partial). Maybe $\alpha_{\rm hot}$ always remains constant at ~ 0.1, while $\alpha_{\rm cold}$ varies by about a factor of 2–3 depending on the strength of the magnetic field from the secondary. This could account for the fact that dwarf novae with similar periods often have quite different outburst timescales. In U Gem, for instance, a system with a somewhat

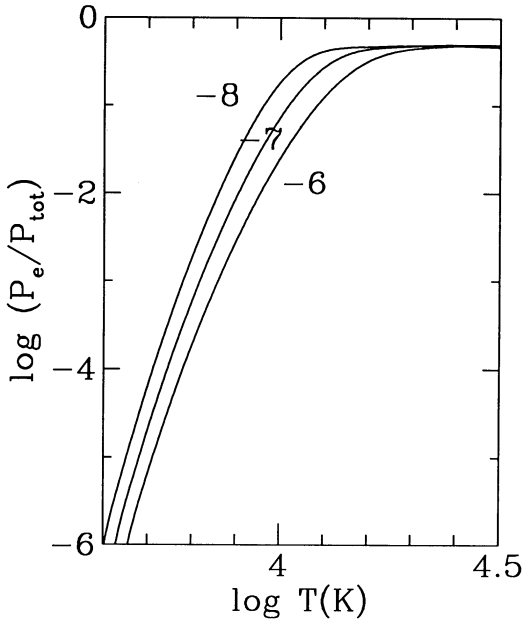

FIG. 16.—The ratio of electron pressure to total pressure vs. temperature for $\log \rho = -8$, -7, and -6 as given by the subroutine PEDET. On the upper branch of the S-curve of allowed steady state solutions for the accretion disk (i.e., $T \gtrsim 40{,}000$ K), the gas is always totally ionized, while in quiescence the degree of partial ionization is a steep function of temperature.

shorter orbital period than SS Cyg, the mean recurrence time is about 120 days, whereas for SS Cyg it is about 50 days. As we have just seen, changes in $\dot{M}_T$ could not directly cause changes in t_c, and since U Gem has a shorter orbital period and presumably a smaller disk, the recurrence time for outbursts would be shorter if $\alpha_{\rm cold}$ and $\alpha_{\rm hot}$ were the same as in SS Cyg. In the scenario we have been discussing, however, the longer recurrence time for U Gem could be explained perhaps by a weaker secondary star magnetic field, leading to a smaller value of $\alpha_{\rm cold}$. Previous workers have noted long-term changes in dwarf novae and interpreted them as being caused by magnetic cycles in the secondary star (e.g., Warner 1988; Bianchini 1990). An alternative explanation suggested by the results shown in Figure 7 is that the α values are the same, and that $r_{\rm inner}$ is different between the two systems. A larger inner disk radius gives a longer recurrence time. Also, the timescales in the disk are related to the local Keplerian orbital period which scales as $\sqrt{r^3/M_{\rm WD}}$, so differences in $M_{\rm WD}$ from system to system would have some effect too.

The results shown in Figure 9 may have implications for the SU UMa systems. Ichikawa, Hirose, & Osaki (1993) model the observed sequence of many short outbursts followed by a long outburst in the SU UMa systems. They find that the dwarf nova outbursts in these systems are all "short"—i.e., there is no viscous plateau and the disk mass increases steadily during the course of several outbursts. At some point the outer edge of the disk has expanded beyond the 3:1 orbital resonance, at which point the tidal torque on the disk should increase. This is accomplished in their model by a sudden, ad hoc, factor of 20 increase in the torque. This brings about a "long" outburst with a viscous plateau that decreases the disk mass substantially and reduces the outer disk radius to a value below that of the 3:1 resonance. The cycle starts over again at this point with another series of short outbursts. We have shown that it

appears to be a natural consequence of the disk limit cycle model to have sequences of outbursts in which some number n of short bursts are sandwiched between two long ones. In SS Cyg, n is usually 1, 2, or 3 (CM). In systems with much lower $\dot{M}_T$, however, n could be much larger. Thus the observed sequencing in the SU UMa systems might also be a natural consequence of their lower mass transfer rates. On the other hand, the 3:1 resonance also seems to play a role, so the two effects might operate together. Also, we have not yet included the effects of tidal torque by the secondary star on the outer edge of the accretion disk, and this affects the outburst characteristics in the SU UMa systems—e.g., the recurrence time increases during the sequence of short ("normal") outbursts lying between two superoutbursts because the matter in the outer disk is spreading to larger radii (Ichikawa et al. 1993).

CSW attempted to formulate analytical expressions for the recurrence time t_c and outburst duration t_b for dwarf nova outbursts. It is useful to see how our time dependent results compare with those of CSW. One of the complications which makes a direct comparison of our two studies somewhat difficult is the fact that we obtain a bimodal distribution of outburst durations. CSW implicitly assumed in their analytical model that, at the beginning of all outbursts, $\Sigma(r_{\rm outer}) = \Sigma_{\rm min}(r_{\rm outer})$. Therefore, all outbursts would have the same duration. In our computations, if we measure t_c from a given point in the outburst—e.g., the crossing of $m_v = 11$ during the rise—then the value of t_c is affected by whether that outburst is long or short. We may obtain a crude estimate of t_c for a given part of a light curve by averaging over both short and long outbursts in the region of interest. For our computation shown in Figure 9, we see that there is virtually no dependence of recurrence time on $\dot{M}_T$. As mentioned previously, this occurs because we always have "inside-out" bursts, where the triggering agent is the viscous drift of material in quiescence and not the direct piling-up of material at large radii. As regards the α dependencies, CSW found $t_c \propto \alpha_{\rm cold}^{-1.23}\alpha_{\rm hot}^{0.34}$. How does this compare with our results? In Figure 10 we increase $\alpha_{\rm cold}$ by a factor of 2, and t_c goes from ~ 80 days to ~ 27 days. In Figure 11 we increase $\alpha_{\rm hot}$ by a factor of 2, and t_c goes from ~ 37 days to ~ 52 days. As a crude scaling we therefore infer $t_c \propto \alpha_{\rm cold}^{-1.5}\alpha_{\rm hot}^{0.5}$—in rough agreement with CSW. For the outburst duration, CSW found t_b to be proportional to $\alpha_{\rm hot}^{-0.8}$ and independent of $\alpha_{\rm cold}$. Since CSW were not considering the long "viscous plateau"–type outbursts, this scaling should be compared to one based on our short outbursts. For the computations shown in Figures 10 and 11 we see that, for the run in which $\alpha_{\rm cold}$ varies, t_b(short) remains constant at ~ 9 days, while for the run in which $\alpha_{\rm hot}$ varies, t_b(short) decreases from ~ 10 days to ~ 7. Therefore $t_b \propto \alpha_{\rm hot}^{-0.5}$—again similar to CSW.

Warner (1987) found many interesting systematic trends by looking at the outburst properties of dwarf novae. Of particular interest, the absolute visual magnitude of the accretion disk at the peak of an outburst (corrected for inclination) appears to be a well-defined, uniformly increasing function of orbital period. In hindsight, one might have predicted this from theory. In quiescence, the disk can only be filled up to a level determined by $\Sigma_{\rm max}$, and so the maximum luminosity of the disk—which is set by the accretion rate in the high state—is limited by the amount of fuel available. CSW established the concept of a "maximum mass"

$$M_{\rm max} = \int_0^{r_{\rm outer}} 2\pi r\,\delta r \Sigma_{\rm max}\,. \tag{19}$$

This is the theoretical maximum amount of material that a disk could store in quiescence before $\Sigma_{\rm max}$ would be exceeded. In practice, $M_{\rm max}$ overestimates somewhat the true disk mass. From the earlier plots showing the evolution of $\Sigma(r, t)$ for example, we see that Σ is much less than $\Sigma_{\rm max}$ near $r_{\rm outer}$ when a burst is triggered. Using our model parameters $r_{\rm outer} = 4 \times 10^{10}$ cm and $\alpha_{\rm cold} = 0.02$, gives $M_{\rm max} = 4.7 \times 10^{24}$ g, while the actual mass at the end of quiescence is seen from the figures showing disk mass versus time to be about 2×10^{24} g. Thus, in SS Cyg the disk is filled to about 40% of its maximum. (This number is probably a function of $r_{\rm add}/r_{\rm outer}$ and so may be different in other models.) We may obtain a simple estimate for the rate of accretion in the disk during the viscous plateau stage of the flat-topped outbursts. We assume that the entire disk is in the hot, ionized state, and that the relevant opacity law is $\kappa = 2.8 \times 10^{24}\rho T^{-3.5}$ cm^2 g^{-1}. Using equation (A3) from Cannizzo & Reiff (1992) then gives

$$\Sigma(\alpha, m_1, r, \dot{M}, \mu) = 40.5 \text{ g cm}^{-2}\,\alpha_{\rm hot,-1}^{-0.8} m_1^{0.25} r_{10}^{-0.75} \dot{M}_{-10}^{0.7} \mu_{\rm hot}^{0.75}\,, \tag{20}$$

where $\dot{M}_{-10}$ is the mass accretion rate within the disk in units of $10^{-10}\ M_\odot$ yr^{-1}. If we take the disk mass to be $fM_{\rm max}$, substitute equation (20) into equation (19), invert for $\dot{M}$, and scale to SS Cyg parameters, we obtain

$$\dot{M} = 1.1 \times 10^{-8}\ M_\odot \text{ yr}^{-1} \left(\frac{\alpha_{\rm hot}}{0.1}\right)^{1.14} \left(\frac{\alpha_{\rm cold}}{0.02}\right)^{-1.23} \times \left(\frac{r_{\rm outer}}{4 \times 10^{10}}\right)^{2.57} \left(\frac{f}{0.4}\right)^{1.43}, \tag{21}$$

consistent with the accretion rates for the flat-topped bursts seen in the fourth panel of Figure 13. The value of $\sim 10^{-8}\ M_\odot$ yr^{-1} for the accretion rate in the disk at maximum light is somewhat lower than values obtained from earlier modelling. From his spectral fitting, Kiplinger (1979) determined a value $\dot{M} \simeq 8.5 \times 10^{-8}\ M_\odot$ yr^{-1}. The rate of increase in $\dot{M}$ (and hence the accretion disk luminosity) with other disk radius which we derive in equation (21) seems to be somewhat steeper than that inferred from Warner's M_v(max)–$P_{\rm orbital}$ relation. This may indicate that f is not constant, but in fact decreases with orbital period. A resolution of this problem must await further computations.

6. CONCLUSION

We have performed time-dependent computations for the accretion disk limit cycle model using variable input parameters. Our computational findings can be summarized as follows:

1. The sequence of alternating long and short outbursts, or of long outbursts separated by several short outbursts, is a natural consequence of the model. These sequences are also commonly seen in SS Cyg. Whether an outburst will be long or short depends on the mass present in the disk at the onset of thermal instability.

2. In order to resolve adequately the transition fronts we find that $\gtrsim 100$ grid points are needed. Coarser zoning leads to spuriously slow outburst timescales (for both t_c and t_b).

3. The recurrence time t_c and the sequencing depend sensitively on the inner disk radius. As $r_{\rm inner}$ is made to increase, t_c increases, $t_b(S)$ decreases, and fewer short outbursts occur between two successive long outbursts. The duration of long

outbursts t_b(L) shows no apparent trend with increasing r_{inner}. The average values of t_b(L) in Figure 7 are (*top to bottom*) ~25 days, ~23 days, ~25 days, ~22 days, and ~22 days, respectively.

4. As r_{outer} is made to increase, more short outbursts occur between two successive long outbursts. The times t_q, $t_b(S)$, and t_b(L) increase weakly with increasing r_{outer}.

5. As the secondary mass transfer rate $\dot{M}_T$ is made to increase, fewer short outbursts occur in a given time interval [i.e., N(L)/N(S) increases], $f_v(q)$ remains constant, t_b(L) increases, t_b(S) remains constant, and, for our input physics, t_q is constant. Ichikawa & Osaki (1993) have shown that the correlation between $\dot{M}_T$ and N(L)/N(S) also holds for models in which t_q and t_c vary inversely with $\dot{M}_T$.

6. As α_{cold} increases (and α_{hot} remains constant), $f_v(q)$ increases, t_q decreases, t_b(L) decreases, t_b(S) remains constant, and N(L)/N(S) decreases. The dependencies of t_c and t_b on α_{cold} are in agreement with CSW.

7. As α_{hot} increases (and α_{cold} remains constant), $f_v(q)$ decreases, t_q increases, t_b(L) decreases (weakly), t_b(S) decreases, and N(L)/N(S) increases. The dependencies of t_c and t_b on α_{hot} are in agreement with CSW.

Our observational findings can be summarized as follows:

In the light curve of SS Cyg, we see fluctuations in the long-term moving averages for t_c, t_q, t_b(L), t_b(S), N(L)/N(S), and ϵ—the fraction of time spent at brighter than 9th mag (and therefore an indicator of the fraction of time spent on a flat-topped outburst, and hopefully, of $\langle \dot{M}_T \rangle$). By looking at the correlations between fluctuations in these quantities we find the following:

1. There is a direct correlation between $\langle t_c \rangle$ and $\langle N(L)/N(S) \rangle$.
2. There is also a direct correlation between $\langle t_q \rangle$ and $\langle N(L)/N(S) \rangle$.
3. There is an inverse correlation between $\langle t_b(L) \rangle$ and $\langle N(L)/N(S) \rangle$.
4. There is no significant correlation between $\langle t_b(S) \rangle$ and $\langle N(L)/N(S) \rangle$.
5. CM already noted an inverse correlation between $\langle t_c \rangle$ and $\langle f_v(q) \rangle$—the moving average of the quiescent visual flux.
6. In addition, there is no obvious correlation between ϵ and anything else.

On the basis of the observed correlations and our computational results, we can place constraints on which parameter(s) may vary so as to produce the observed fluctuations. We have identified five parameters: r_{inner}, r_{outer}, $\dot{M}_T$, α_{cold}, and α_{hot}. Let us discuss each in turn.

r_{inner}.—In Figure 7 we see a direct correlation (1) between t_c and N(L)/N(S), and (2) between t_q and N(L)/N(S). There is no correlation (3) between t_b(L) and N(L)/N(S). There is an inverse correlation (4) between t_b(S) and N(L)/N(S) and (5) between t_c and $f_v(q)$. Thus (1), (2), and (5) are in accord with observations, while (3) and (4) are not.

r_{outer}.—In Figure 8 we see inverse correlations (1) between t_c and N(L)/N(S), (2) between t_q and N(L)/N(S), (3) between t_b(L) and N(L)/N(S), and (4) between t_b(S) and N(L)/N(S). There is no correlation (5) between t_c and $f_v(q)$. Thus (3) is in accord with observations, while (1), (2), (4) and (5) are not.

$\dot{M}_T$.—In Figure 9 we see a direct correlation between $\dot{M}_T$ and N(L)/N(S). As discussed earlier, in our models we have only inside-out outbursts so that $t_c \neq t_c(\dot{M}_T)$. Ichikawa & Osaki (1993) have shown, however, that N(L)/N(S) also scales with $\dot{M}_T$ for models in which t_c varies inversely with $\dot{M}_T$. In our model we also find a direct correlation between t_b(L) and N(L)/N(S), and no correlation between t_b(S) and N(L)/N(S). The only variation that agrees with the observed ones is that between t_b(S) and N(L)/N(S).

α_{cold}.—In Figure 10 we see direct correlations (1) between t_c and N(L)/N(S), (2) between t_q and N(L)/N(S), and (3) between t_b(L) and N(L)/N(S). There is no correlation (4) between t_b(S) and N(L)/N(S), and an inverse correlation (5) between t_c and $f_v(q)$. Thus (1), (2), (4), and (5) are in accord with observations, while (3) is not.

α_{hot}.—In Figure 11 we see a direct correlation (1) between t_c and N(L)/N(S) and (2) between t_q and N(L)/N(S). There is a weak inverse correlation (3) between t_b(L) and N(L)/N(S), and also an inverse correlation (4) between t_b(S) and N(L)/N(S), and (5) between t_c and $f_v(q)$. Thus (1), (2), (3), and (5) are in accord with observations, while (4) is not.

It appears unlikely that fluctuations in $\dot{M}_T$ could produce the long-term changes seen in SS Cyg in the manner envisioned by HK90 and CM. Even if we had adjusted our input physics so as to produce outside-in bursts and thereby obtain *some* dependence of t_c on $\dot{M}_T$, the correlation between t_c and N(L)/N(S) would have been an inverse one, instead of a direct one as observed. If the accretion disk viscosity or the inner disk radius were mediated by changes in $\dot{M}_T$, then changes in $\dot{M}_T$ could *indirectly* account for the observed correlation between $\langle t_c \rangle$ and $\langle N(L)/N(S) \rangle$ [and between $\langle t_q \rangle$ and $\langle N(L)/N(S) \rangle$] (1) if r_{inner} were inversely related to $\dot{M}_T$, or (2) if α_{cold} were inversely related to $\dot{M}_T$ and α_{hot} were constant, or (3) if α_{hot} were directly related to $\dot{M}_T$ and α_{cold} were constant. The constraint that one of the two α's remain fixed is forced on us by the fact that the changes in the sequencing and quiescent light level from the disk brought about by changes in α's work oppositely. If both α's were varying coherently, then their combined effects would nearly cancel out as regards changes in the sequencing of long and short outbursts. Given the lack of correlation between ϵ and any other quantity in Figure 14, however, the motivation for a mass transfer induced effect seems weak.

A second option is that some other physical property associated with the secondary star influences the viscosity—perhaps a magnetic field threading the outer edge of the disk. Tout & Pringle (1992) discuss a dynamo model which combines the Balbus & Hawley and Parker instabilities. In this model, a seed field is amplified to rough equipartition with the gas pressure. In the low state of the disk, however, the extreme sensitivity of the partial ionization of the gas on temperature may affect the efficiency of the shear amplification. Therefore, α_{hot} might be a universal constant, while α_{cold} might vary to some degree with fluctuations in the magnetic field from the secondary star.

A third option is that both α_{cold} and α_{hot} are constant and that variations occur in $\langle r_{inner} \rangle$—the mean value of the inner disk radius. While this could account for the transition from LS to LSS behavior in terms of the change in recurrence times observed in SS Cyg (i.e., about 40 days for LSS and about 60 days for LS), it would be difficult to account for times during which only long outbursts occur, because the predicted recurrence time would be much longer than observed.

The variation of no one parameter appears capable of accounting for all five of the observed correlations mentioned earlier. Variations in α_{cold} and α_{hot} produce correlated changes which agree with all but one of those observed, while variations in r_{inner} agree with all but two. The disagreements involve the durations of either the long or short outbursts: r_{inner} variations produce an inverse correlation between t_b(S) and N(L)/

N(S) (rather than no correlation) and no correlation between t_b(L) and N(L)/N(S) (rather than an inverse correlation); α_{cold} variations produce a direct correlation between t_b(L) and N(L)/N(S) (rather than an inverse correlation); and α_{hot} variations produce an inverse correlation between t_b(S) and N(L)/N(S) (rather than no correlation). It is not clear how serious these disagreements are. For example, one curious feature seen in Figure 15 concerns the cross-correlation function between $\langle t_b(\mathrm{L})\rangle$ and $\langle N(\mathrm{L})/N(\mathrm{S})\rangle$. The fluctuations in $\langle t_b(\mathrm{L})\rangle$ lead those in $\langle N(\mathrm{L})/N(\mathrm{S})\rangle$ by ~ 300 days. This may indicate the presence of some feedback mechanism. During the time t_b(L) when the disk is entirely in the high state, h/r will be large because of high disk temperatures. This will tend to shield the area around the inner Lagrangian point on the secondary star, perhaps affecting the mass flow. A strong heating effect on the secondary has been seen in SS Cyg (Hessman et al. 1984) during times when the system is on the "viscous plateau." It is not clear how the inclusion of such an effect into our model would change the correlations of the long and short outburst times with N(L)/N(S). In light of this, we view as more noteworthy the correlations of t_c with N(L)/N(S) in the models.

Finally, it appears that long outbursts in SS Cyg and other dwarf novae have very much in common with superoutbursts in the SU UMa stars. It is during these types of outbursts that a substantial fraction of the matter in the accretion disk is accreted onto the white dwarf. During the shorter outbursts—those which rise to maximum and immediately begin to decay back to quiescence—the accretion disk is never entirely in the high state and only a small fraction of the disk accretes onto the WD. One of the differences between the light curves of systems such as SS Cyg above the period gap and those such as VW Hyi below the gap is the number n of short outbursts lying between two successive long outbursts. In SS Cyg, $n \sim 1$–3, whereas in VW Hyi, $n \sim 5$–10. This may be a natural consequence of the lower rates of mass transfer in the shorter orbital period systems.

It is a pleasure to acknowledge stimulating conversations with Brian Warner and Craig Wheeler. I also thank Janet Mattei for permission to use the AAVSO data on SS Cyg. This research was supported by the National Academy of Sciences through a National Research Council associateship.

REFERENCES

Allen, C. W. 1983, Astrophysical Quantities (London: Athlone)
Balbus, S. A., & Hawley, J. F. 1991, ApJ, 376, 214
Bath, G. T., & Pringle, J. E. 1981, MNRAS, 194, 967
———. 1982, MNRAS, 199, 267
Bianchini, A. 1990, AJ, 99, 1941
Cannizzo, J. K. 1984, Nature, 311, 443
———. 1992, ApJ, 385, 94
———. 1993, in Accretion Disks in Compact Stellar Systems, ed. J. C. Wheeler (Singapore: World Scientific), in press
Cannizzo, J. K., Ghosh, P., & Wheeler, J. C. 1982, ApJ, 260, L83
Cannizzo, J. K., & Kenyon, S. J. 1986, ApJ, 309, L43
———. 1987, ApJ, 320, 319
Cannizzo, J. K., & Mattei, J. A. 1992, ApJ, 401, 642 (CM)
Cannizzo, J. K., & Pudritz, R. E. 1988, ApJ, 327, 840
Cannizzo, J. K., & Reiff, C. M. 1992, ApJ, 385, 87
Cannizzo, J. K., Shafter, A. W., & Wheeler, J. C. 1988, ApJ, 333, 227 (CSW)
Cannizzo, J. K., & Wheeler, J. C. 1984, ApJS, 55, 367 (CW)
Cannizzo, J. K., Wheeler, J. C., & Polidan, R. S. 1986, ApJ, 301, 634
Duschl, W. J., & Livio, M. 1989, A&A, 209, 183 (DL)
Fabbiano, G., Hartmann, L., Raymond, J., Steiner, J., Branduardi-Raymont, G., & Matilsky, T. 1981, ApJ, 243, 911
Faulkner, J., Lin, D. N. C., & Papaloizou, J. 1983, MNRAS, 205, 359 (FLP)
Ghosh, P., & Lamb, F. K. 1977, ApJ, 217, 578
———. 1979a, ApJ, 232, 259
———. 1979b, ApJ, 234, 296
Giovannelli, F., & Martinez-Pais, I. G. 1991, Space Sci. Rev., 56, 313
Hassall, B. J. M., Pringle, J. E., & Verbunt, F. 1985, MNRAS, 216, 353
Hempelmann, A., & Kurths, J. 1990, A&A, 232, 356 (HK90)
———. 1993, ApJ, 412, L41
Hessman, F. V., Robinson, E. L., Nather, R. E., & Zhang, E.-H. 1984, ApJ, 286, 747
Honeycutt, R. K., Cannizzo, J. K., & Robertson, J. W. 1993, ApJ, submitted
Huang, M., & Wheeler, J. C. 1989, ApJ, 343, 229
Iben, I., Jr. 1963, ApJ, 138, 452
Ichikawa, S., Hirose, M., & Osaki, Y. 1993, PASJ, 45, 243
Ichikawa, S., & Osaki, Y. 1992, PASJ, 44, 15
———. 1993, in Theory of Accretion Disks 2, ed. F. Meyer, W. J. Duschl, E. Meyer-Hofmeister, J. Frank, & W. Tscharnuter (Dordrecht: Kluwer), in press
Jones, M. H., & Watson, M. G. 1992, MNRAS, 257, 633
Kiplinger, A. L. 1979, ApJ, 234, 997
Lin, D. N. C., Papaloizou, J., & Faulkner, J. 1985, MNRAS, 212, 105 (LPF)
Livio, M., & Pringle, J. E. 1992, MNRAS, 259, 23P
Meyer, F. 1991, Rev. Mod. Astron., 3, 1
Meyer, F., & Meyer-Hofmeister, E. 1981, A&A, 104, L10
———. 1984, A&A, 132, 143
———. 1989, A&A, 221, 36
Mineshige, S. 1986, PASJ, 38, 831
———. 1988, A&A, 190, 72
Mineshige, S., & Osaki, Y. 1983, PASJ, 35, 377 (MO83)
———. 1985, PASJ, 37, 1
Mineshige, S., & Shields, G. A. 1990, ApJ, 351, 47
Osaki, Y. 1974, PASJ, 26, 429
———. 1989, PASJ, 41, 1005
Pojmański, G. 1986, Acta Astr., 36, 69
Pringle, J. E. 1988, MNRAS, 230, 587
Pringle, J. E., Verbunt, F., & Wade, R. A. 1986, MNRAS, 221, 169
Rosino, L., Romano, G., & Marziani, P. 1993, PASP, 105, 51
Shakura, N. I., & Sunyaev, R. A. 1973, A&A, 24, 337
Smak, J. 1982, Acta Astr., 32, 199
———. 1984, Acta Astr., 34, 161
Szkody, P., Mattei, J. A., Waagen, E. O., & Stablein, C. 1991, ApJS, 76, 359
Tout, C. A., & Pringle, J. E. 1992, 259, 604
Vishniac, E. T., & Diamond, P. 1989, ApJ, 347, 435
———. 1992, ApJ, 398, 561
Vitello, P., & Shlosman, I. 1993, ApJ, 410, 815
Warner, B. 1987, MNRAS, 227, 23
———. 1988, Nature, 336, 129
Wesselink, A. J. 1939, ApJ, 89, 659